

OC415-3 Cruise Report

Draft 9/14/05

Contents

1. Objectives
2. Cruise narrative
3. Summary of VPR deployments, MOCNESS tows, and incubations
4. Comparison of CTD oxygen sensors with Winkler titrations
5. Comparison of CTD fluorescence with extracted pigments
6. VPR Survey of A4
7. Diatom distributions from VPR data
8. Vertical sections from A4 CTD survey
9. Water properties on isopycnal surfaces
10. ADCP data troubleshooting
11. Cruise participants

1. Objectives

Voyage 415-3 of R/V *Oceanus* was the third cruise (“Survey 2”) of the Eddy Dynamics, mixing, Export, and Species composition (EDDIES) project. A detailed description of the EDDIES science plan is contained in the original proposal, available on the project web site¹. A summary of the findings from voyage 415-1 of R/V *Oceanus* (“Survey 1”) is available at the same URL.

The specific objectives of this cruise “Survey 2” were to:

1. Conduct detailed grid survey of target feature cyclone A4 (XBT, ADCP, CTD/Rosette, MOCNESS, VPR, Light probe)
2. Coordinate with R/V *Weatherbird II* in joint sampling operations of target feature A4
3. Resample eddy feature A5 as time allows.

2. Cruise Narrative

August 7

Departed BDA at 0830. Test CTD cast at 1530. Commenced hourly XBT operations at 1900, ca. 100 miles NE of EC.

Drifter deployed during OC415-2 indicates EC located at 30 2.4N 68 3.0W, or 138 n.m. at 078 from our initial observation of EC on 6/26. It has now covered 255km in 42 days for a mean propagation speed of 6 km/day.

¹ http://science.whoi.edu/users/mcgillic/eddies/EDDIES_Project.html

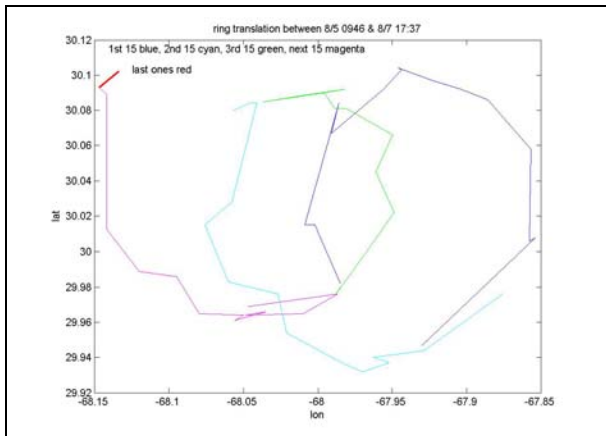


Figure 0807.1: Recent trajectory of drifter deployed on OC415-2.

August 8

ADCP/XBT survey indicates EC bounded by waypoint #s 2072, 2073, 2013, and 2014 (Figures 0808.1,2). VPR deployed for A4 core survey.

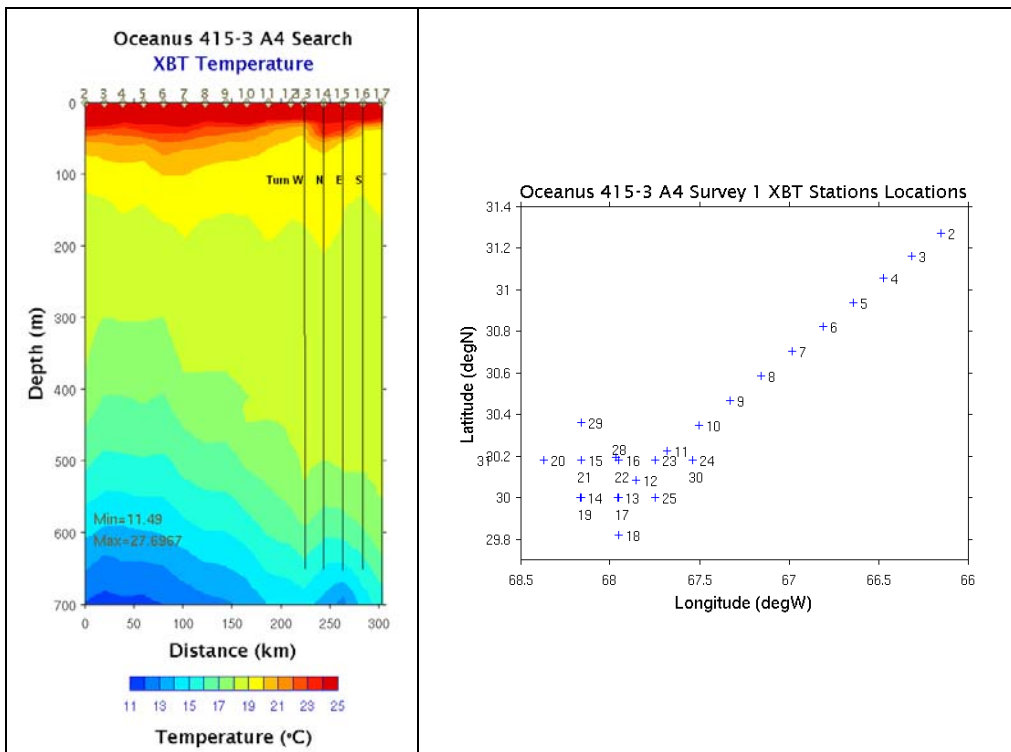


Figure 0808.1: XBT search for A4 center.

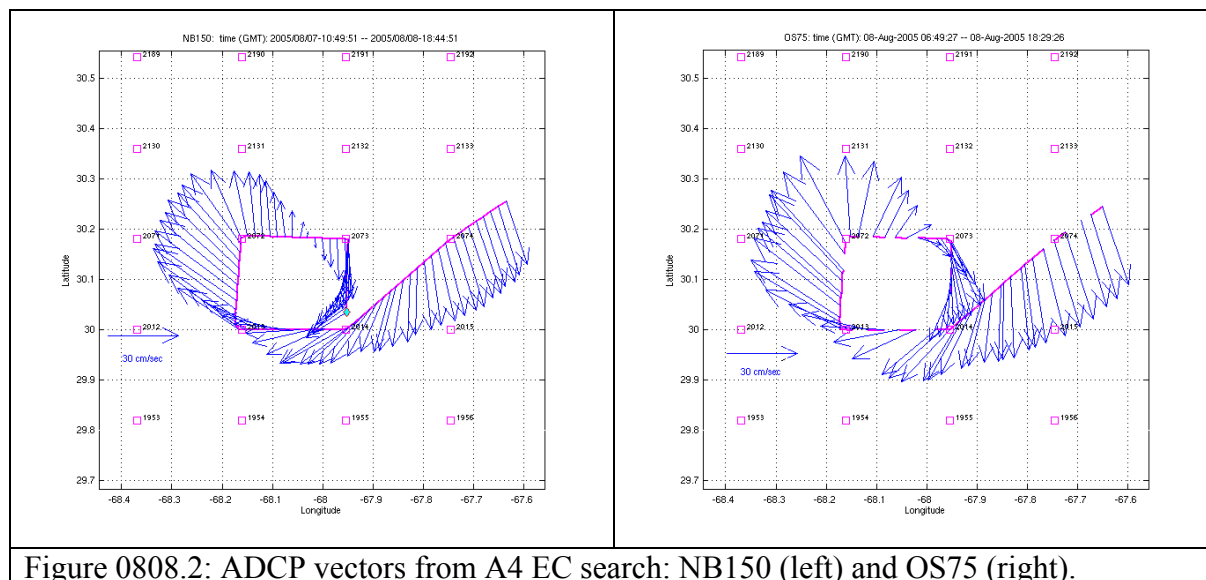


Figure 0808.2: ADCP vectors from A4 EC search: NB150 (left) and OS75 (right).

August 9

VPR recovered due to data dropouts. Camera connector tightened and VPR redeployed. Problem arose again after a few hours, VPR recovered.

CTD grid of A4 inner core begun.

MOCNESS tow at EC 1030 hrs. – quite thick, especially for a daytime tow.

Glider deployed 1630 at WP 2013.

MOCNESS tow at EC 2200 hrs. – very thin.

August 10

CTD grid of inner core completed. None of the nine stations exhibited peaks in fluorescence of the magnitude observed in the first cruise. In contrast, the VPR data reveal fluorescence peaks comparable to those measured during OC415-1 (Figure 0810.1). Moreover, the 20 km resolution of the “high resolution” grid appears to undersample the patches of fluorescence. Therefore a set of three “supplementary” stations (S1-S3, CTD stations 12-14) were occupied at 10km resolution at eddy center. Stations S1-S3 revealed high fluorescence patches, with S3 values peaking in excess of $4 \mu\text{g l}^{-1}$ chl a. Drifter deployed during OC415-2 was ca. 100 yards to starboard during the cast at S3. The fluorescence peak at S3 is higher than any we observed during OC415-1. However, averaged fluorescence over the 60-140m depth interval in the inner core grid is about 25% lower overall in OC415-3 than in OC415-1 (Figure 0810.2). An important caveat to this inter-cruise comparison is undersampling of this very patchy distribution of chlorophyll.

MOCNESS tow at S3 at 2200 hrs.

Incubation cast at S3 yields $4 \mu\text{g l}^{-1}$ chl a on the fluorometer, similar to that observed a few hours earlier at the same station. Microscope counts confirm the presence of chain-forming diatoms (*Chaetoceros* spp.) in the chlorophyll maximum.

See Figure 0811.3 for a complete set of inner core survey maps.

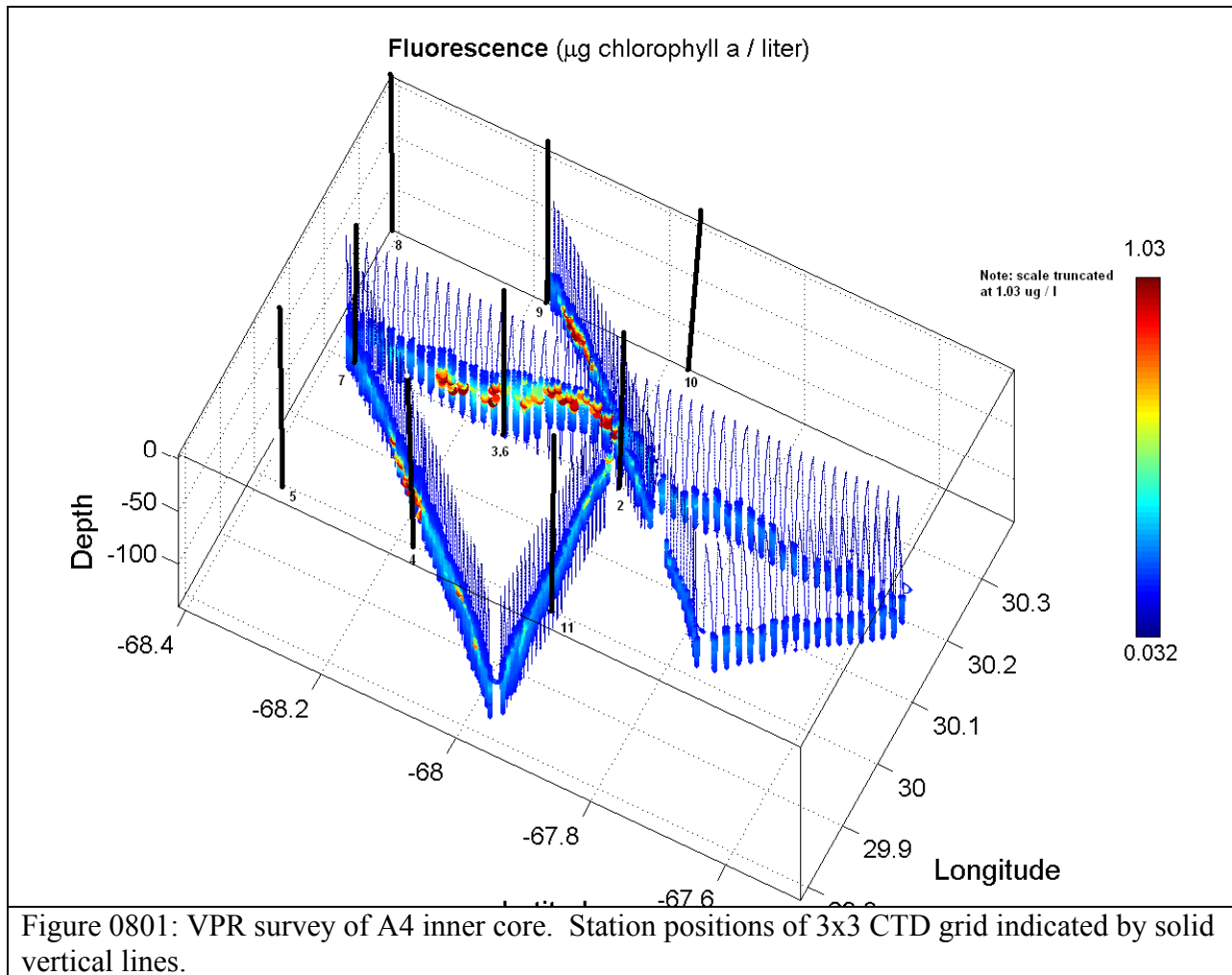


Figure 0801: VPR survey of A4 inner core. Station positions of 3x3 CTD grid indicated by solid vertical lines.

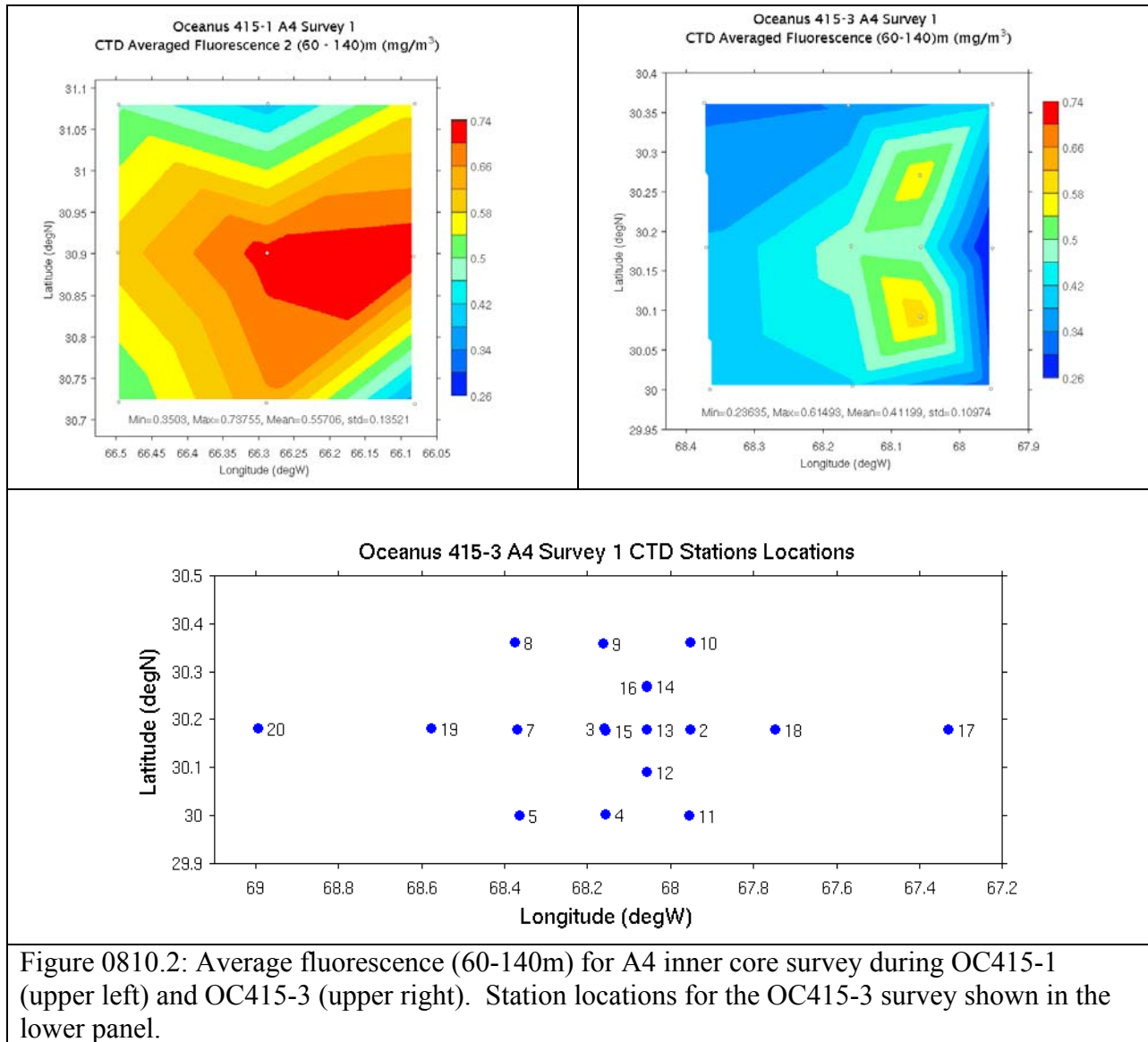
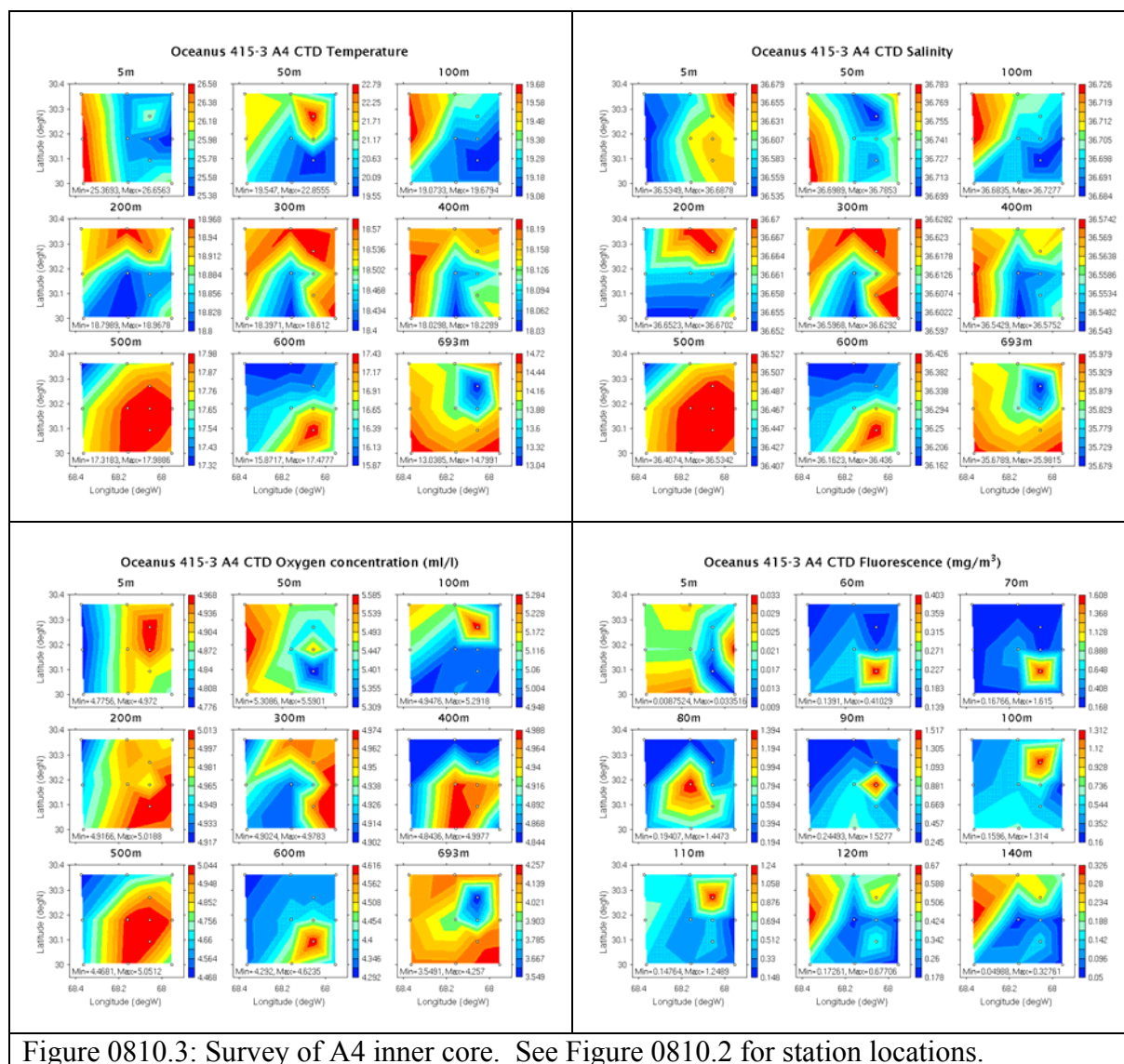


Figure 0810.2: Average fluorescence (60-140m) for A4 inner core survey during OC415-1 (upper left) and OC415-3 (upper right). Station locations for the OC415-3 survey shown in the lower panel.



August 11

E-W CTD transect through A4 completed. Doming of the seasonal thermocline and depression of the main thermocline has a clear impact on all hydrographic variables (Figure 0811.1). Both the nitracline and phosphocline continue to outcrop into the euphotic zone (Figure 0811.2).

An important caveat to interpretation of these maps is the issue of high frequency temporal variability, which can masquerade as spatial variability. Consider the nitrate profiles for the three supplementary stations S1-S3 (CTDs 12-14, Figure 0811.3). Plotted as a function of depth,

these profiles suggest a dramatic change in nutrient availability at the base of the euphotic zone over 10km spatial scales. Plotted as a function of density, the nutrient profiles for these three stations are nearly identical. Thus, high-frequency isopycnal displacements (associated with inertial motions and internal waves) are aliased in these observations.

Despite contamination by high-frequency motions, eddy-driven nutrient enhancement in the core of A4 is a consistent feature of the observations (Figure 0811.4). Interestingly, nitrate availability in the euphotic zone is just as high on OC415-3 as it was during OC415-1. The mechanism responsible for maintaining such high nutrient concentrations in the euphotic zone over such a long period of time is unknown.

TS Irene has strengthened and will make our area of operations in A4 unworkable over the next few days. Therefore we will transit to A5 to make best use of our time. The plan is:

- 1) XBT/ADCP/VPR search for A5 eddy center, estimated at 33 0' 64 45' (Figure 0811.5)
- 2) CTD section across A5
- 3) Return to A4 for Joint Ops with WBII

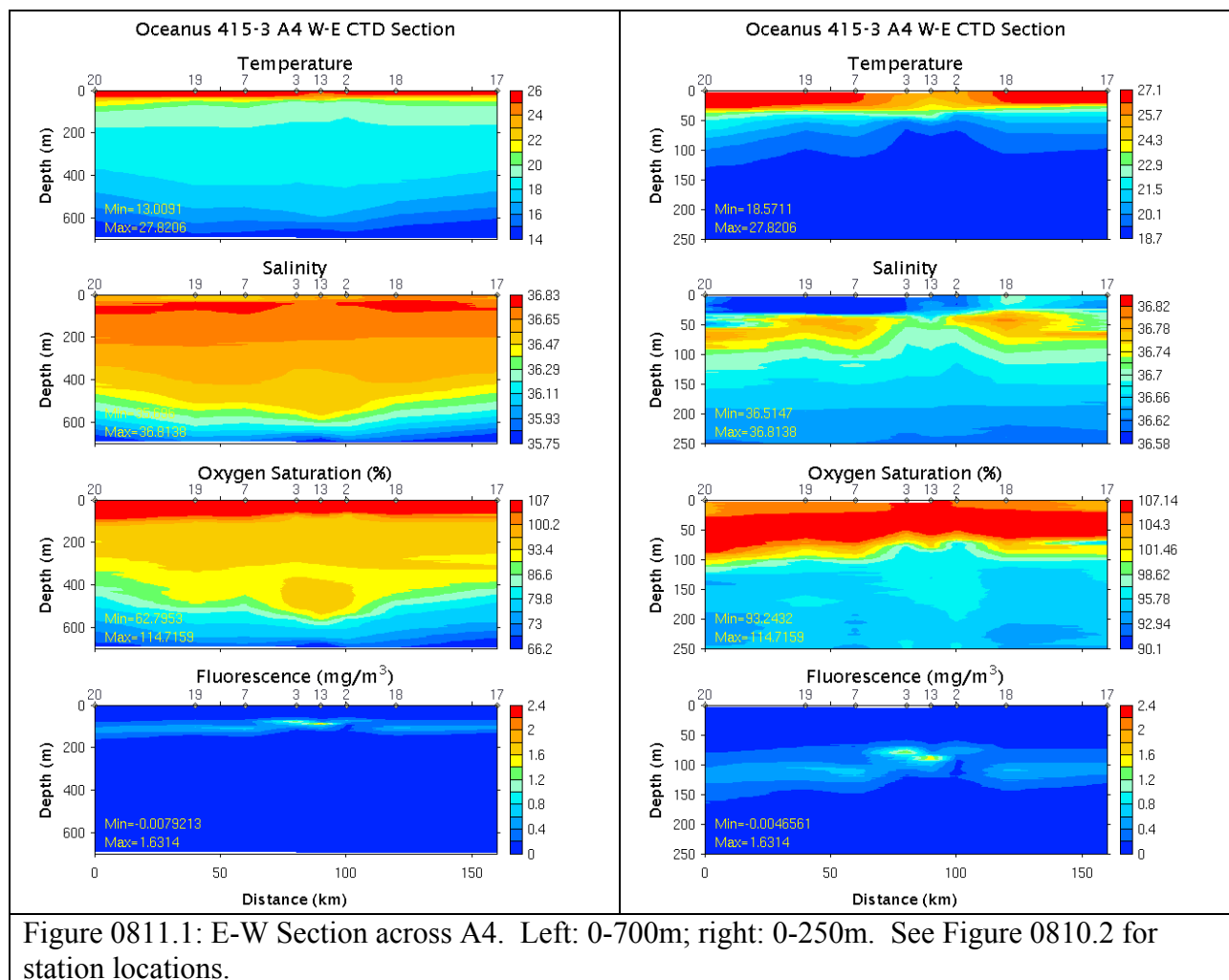


Figure 0811.1: E-W Section across A4. Left: 0-700m; right: 0-250m. See Figure 0810.2 for station locations.

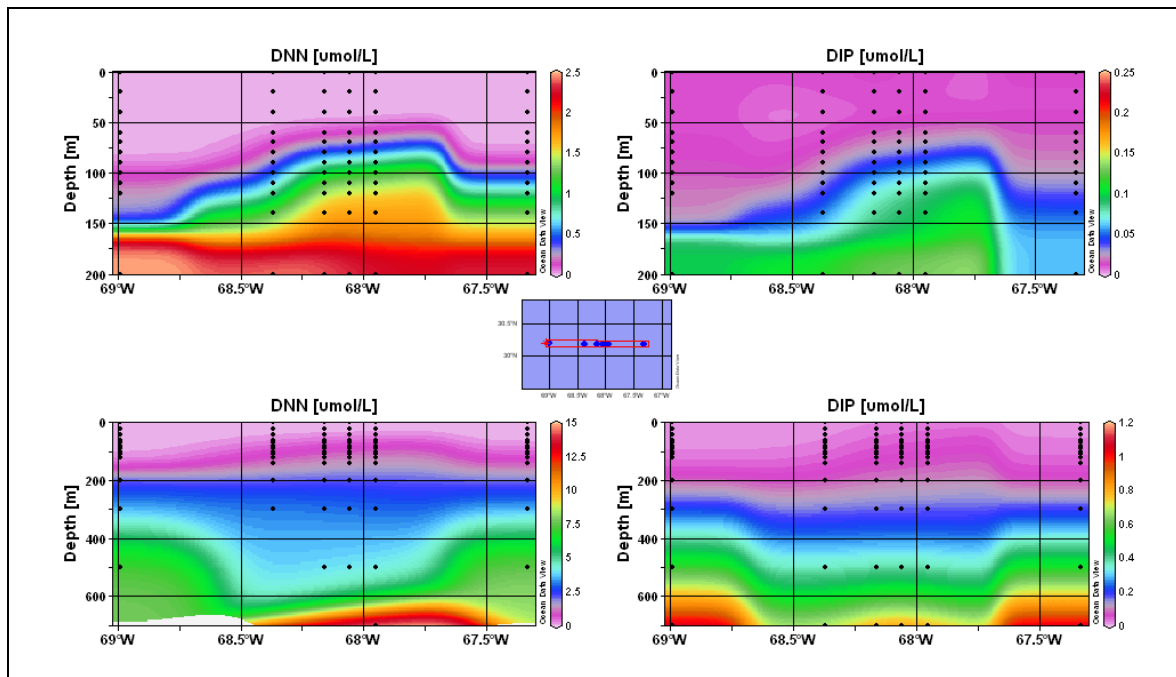


Figure 0811.2: Sections of nitrate (left) and phosphate (right) across A4. Upper and lower panels show 0-200m and 0-700m, respectively.

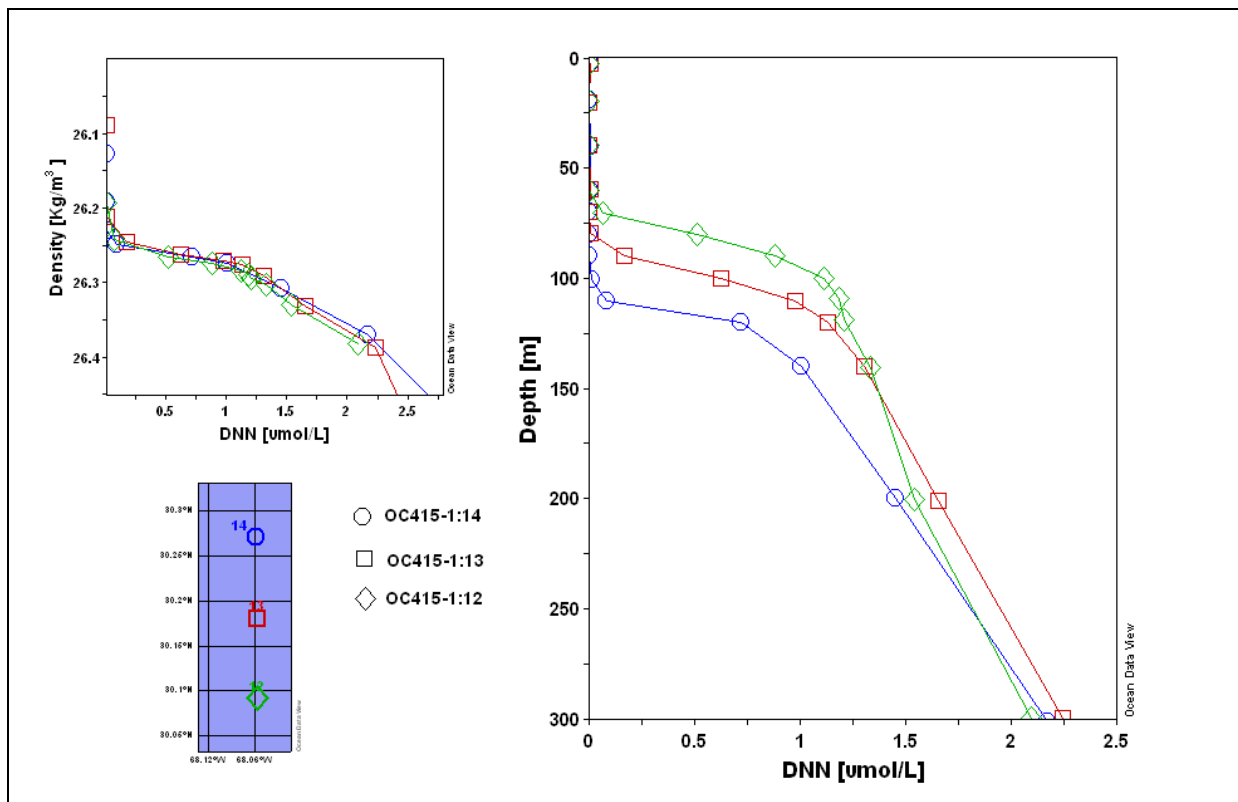


Figure 0811.3: Nitrate profiles for stations S1, S2, and S3 plotted as a function of density (left) and depth (right).

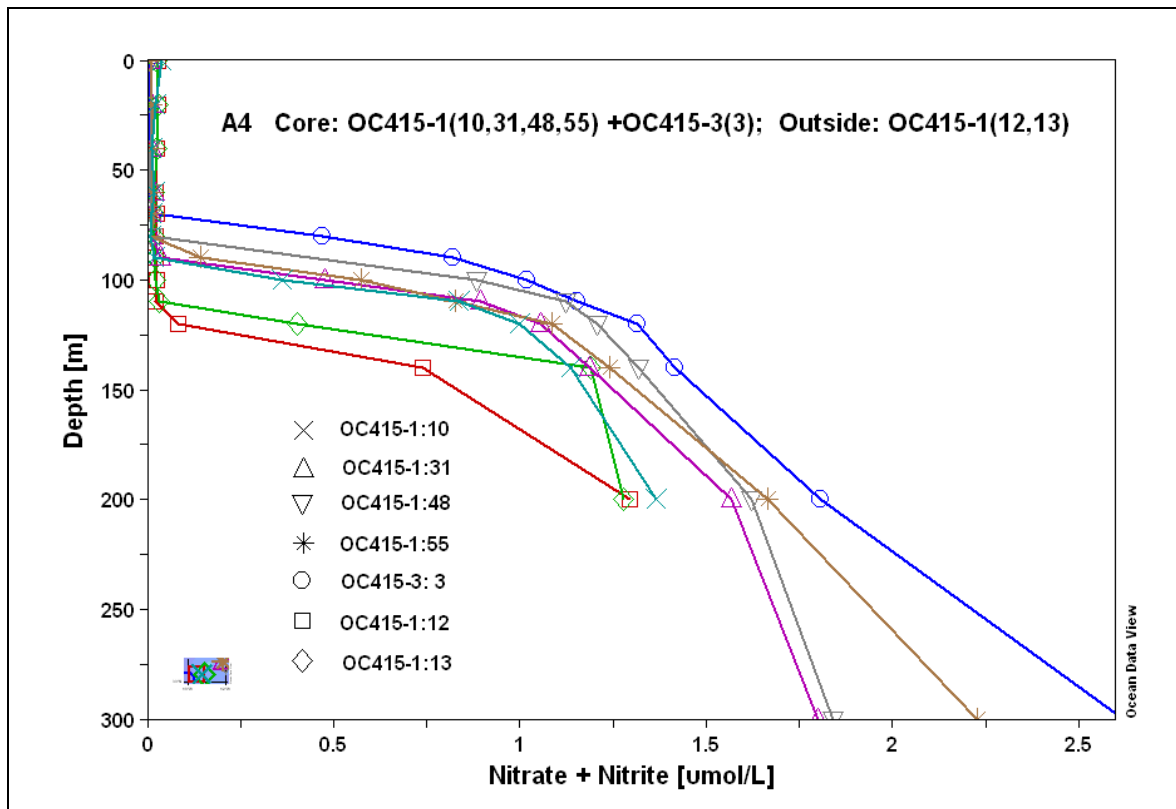


Figure 0811.4: Nitrate profiles inside and outside A4 during OC415-1 and OC415-3. Stations 12 and 13 from OC415-1 are outside the eddy; stations 10, 31, and 48 from OC415-1 are at the center of A4. Station 3 from OC415-3 is at the eddy core. A mean for stations 1-55 of OC415-1 is also shown.

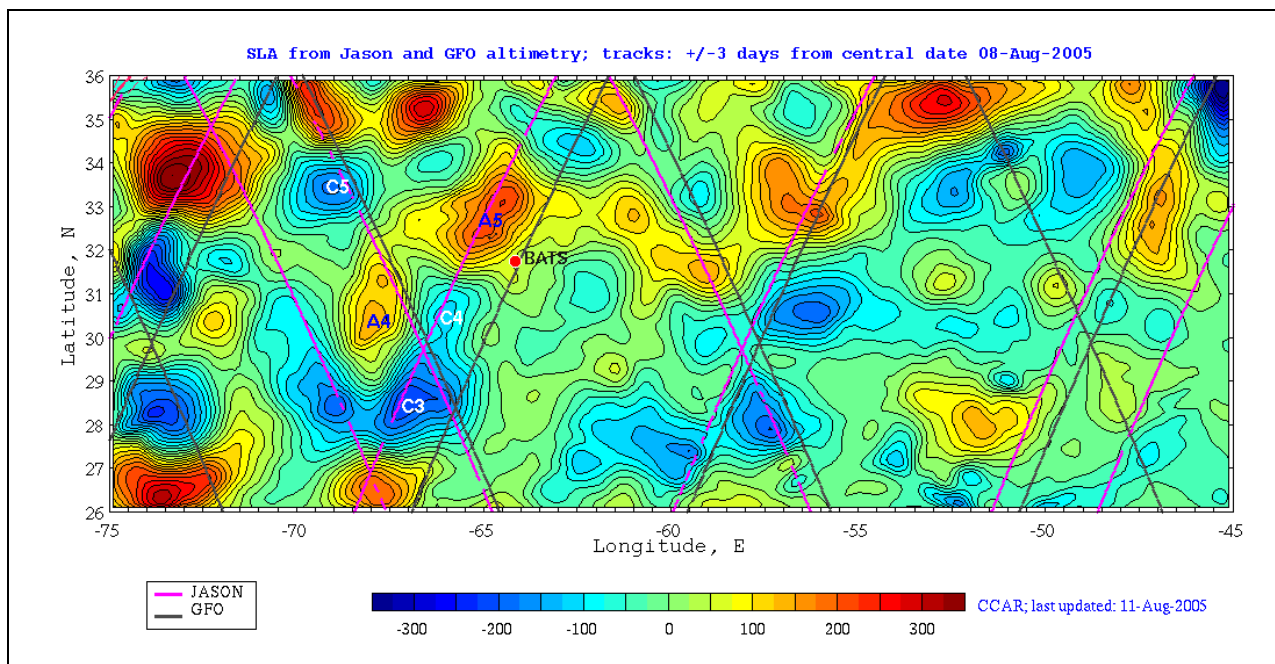
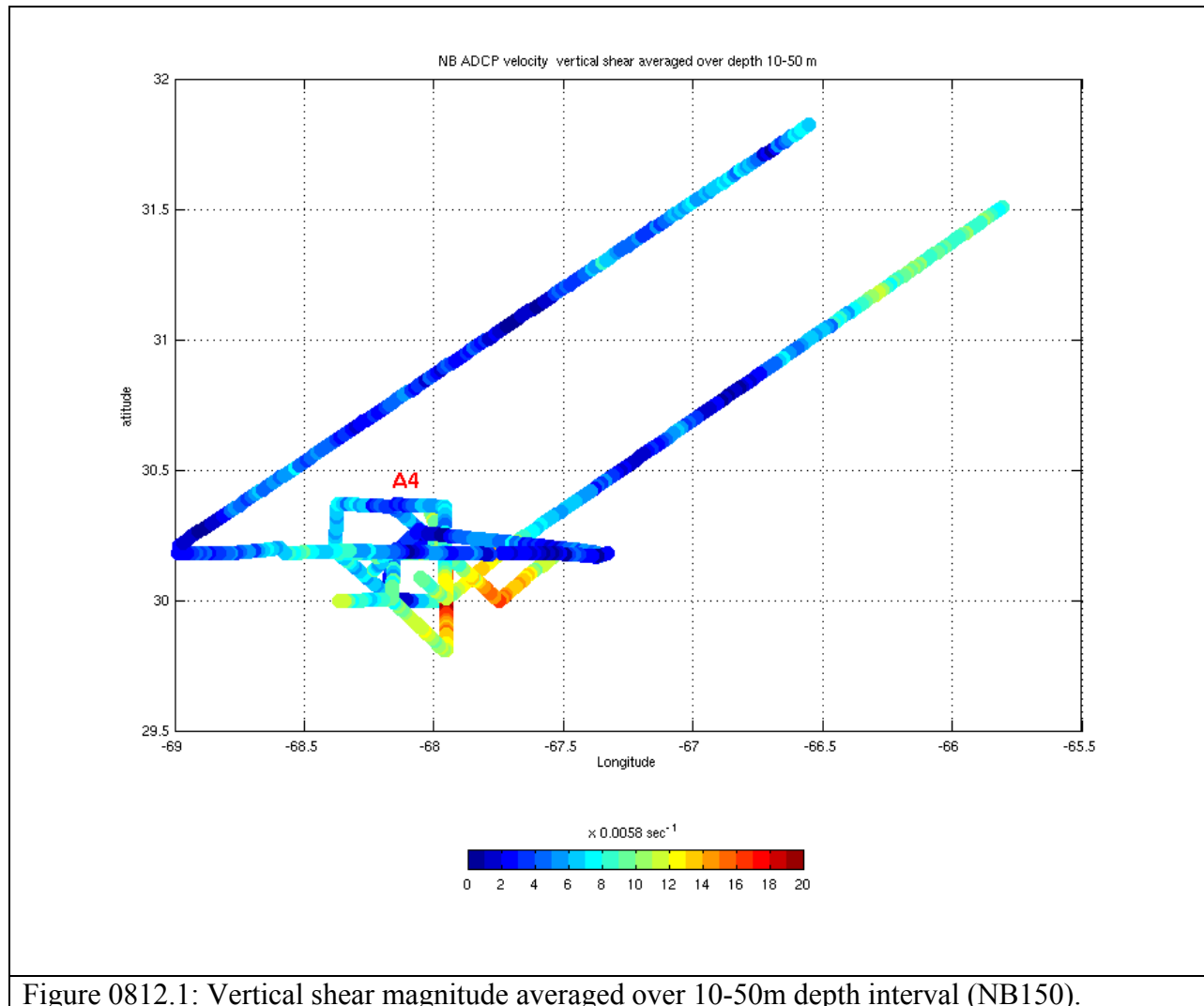


Figure 0811.5: Altimetric objective analysis for August 8. Note new Jason track over A5.

August 12

Transit to A5; begin XBT drops at 0400. VPR ready for deployment at 1215; pre-flight fails due to rudder problem. Turns out to be loose connector. Redeployed later that afternoon, a few hours of good towing before data dropouts begin. VPR rolls on recovery.

Shear from NB150 indicates enhancement associated with A4 (Figure 0812.1)



August 13

Center of A5 located (Figures 0813.1) and CTD transect begun. Night MOCNESS tow at EC.

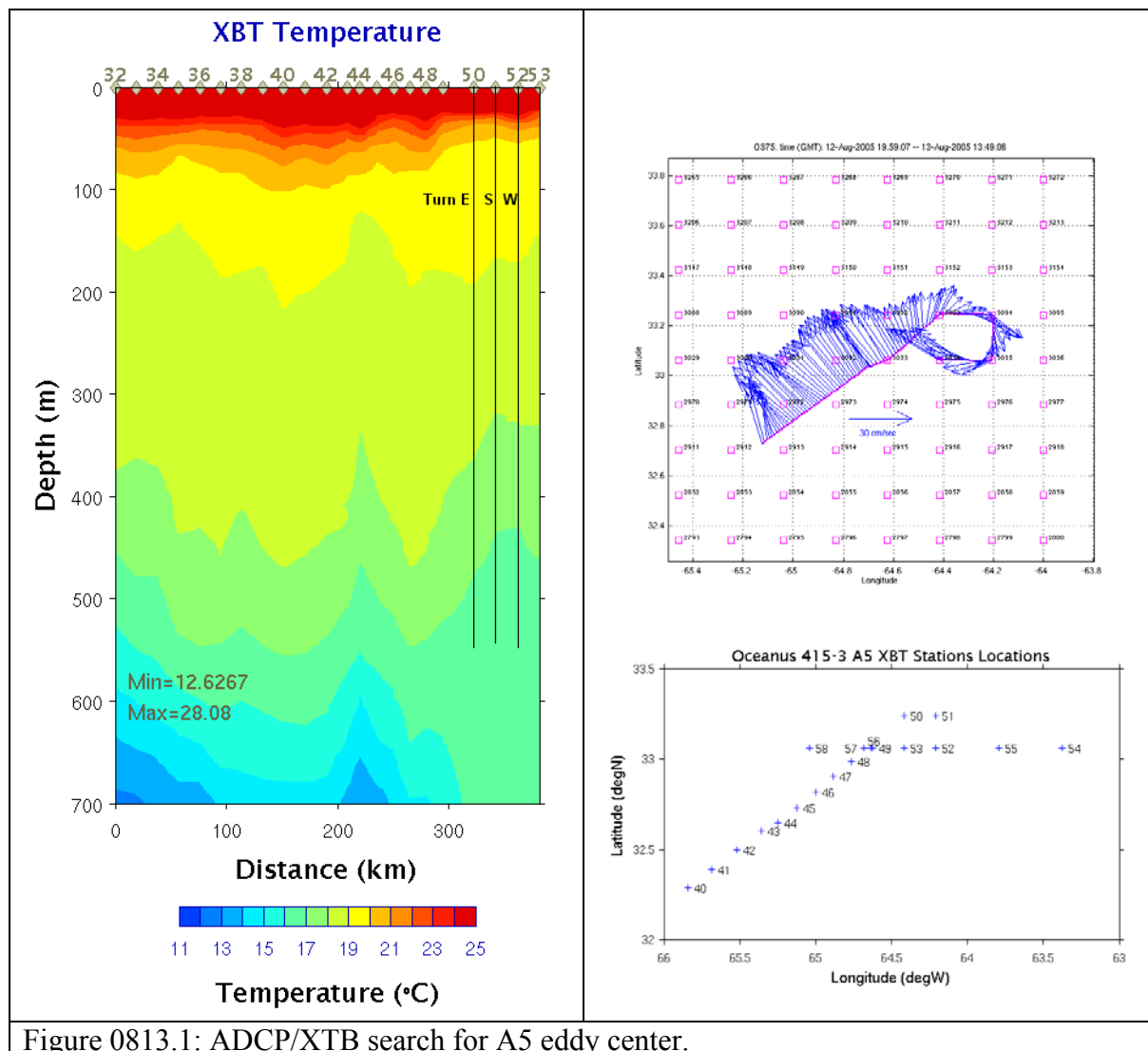


Figure 0813.1: ADCP/XTB search for A5 eddy center.

August 14

CTD transect of A5 completed (Figures 0814.1,2,3). The bolus of 16-degree water clearly domes the seasonal pycnocline and depresses the main pycnocline. Positive oxygen anomaly in the core of the 16-degree water. Fluorescence elevated at eddy center and also on the western edge. Nutrients enhanced at the base of the euphotic zone.

Transit to BDA pilot station for o-ring pickup. Proceed toward A4 EC.

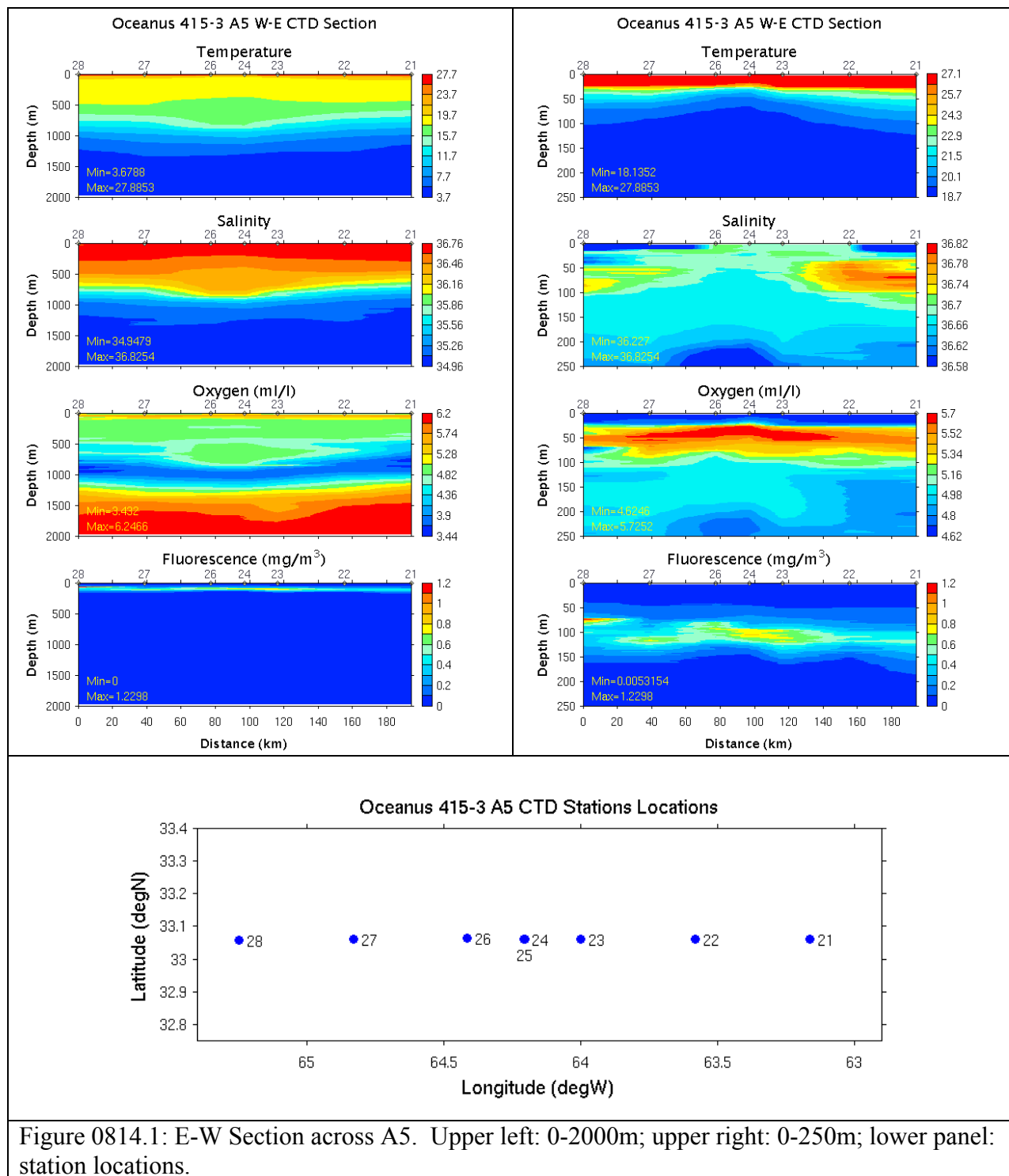


Figure 0814.1: E-W Section across A5. Upper left: 0-2000m; upper right: 0-250m; lower panel: station locations.

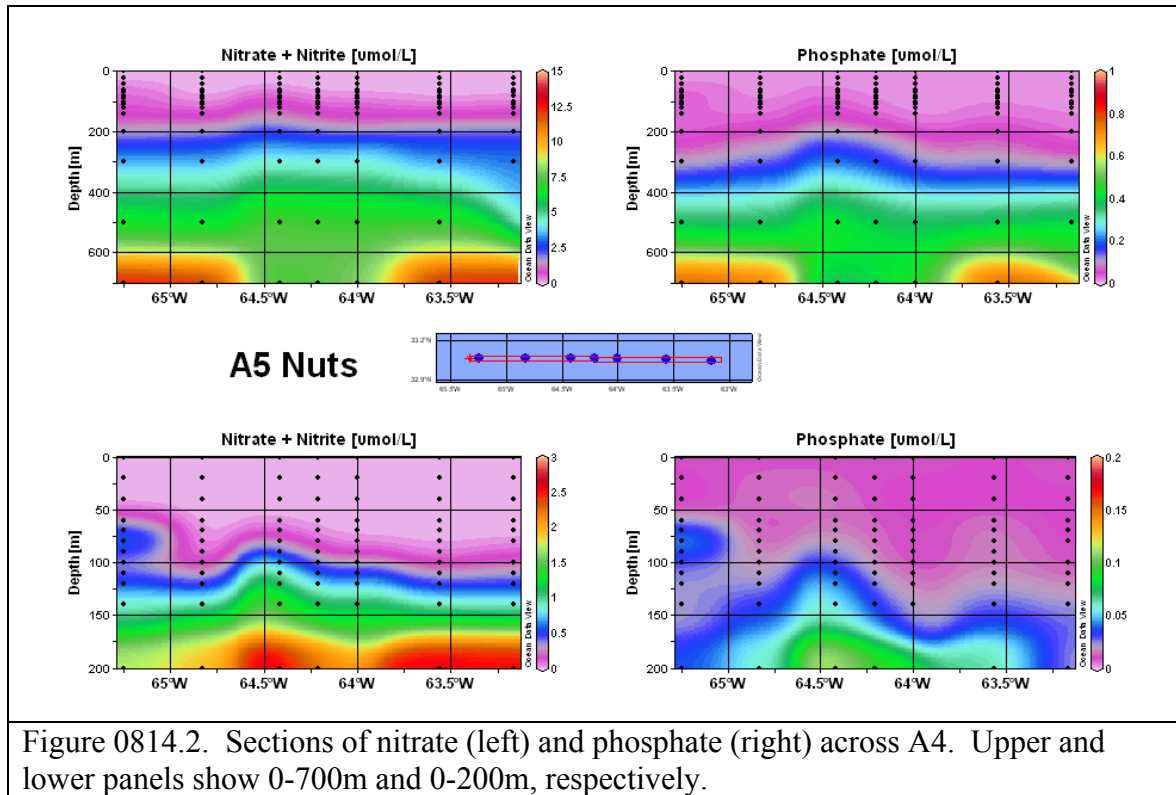


Figure 0814.2. Sections of nitrate (left) and phosphate (right) across A4. Upper and lower panels show 0-700m and 0-200m, respectively.

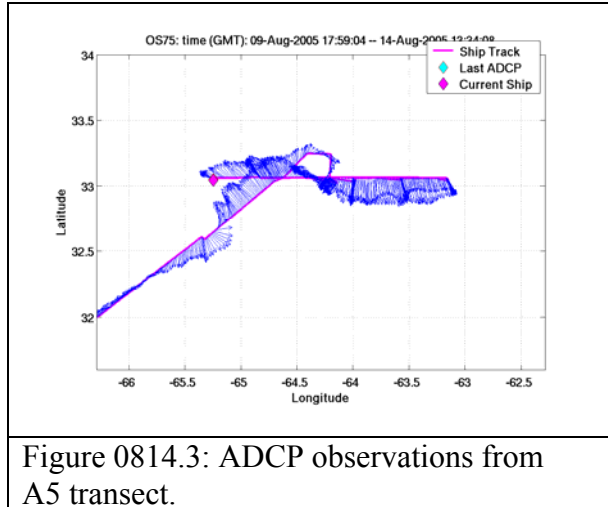


Figure 0814.3: ADCP observations from A5 transect.

August 15

Transit back to A4. XBT drops commence at 0800; VPR deployed at 0830. A4 center located at waypoint 2071 (Figure 0815.1).

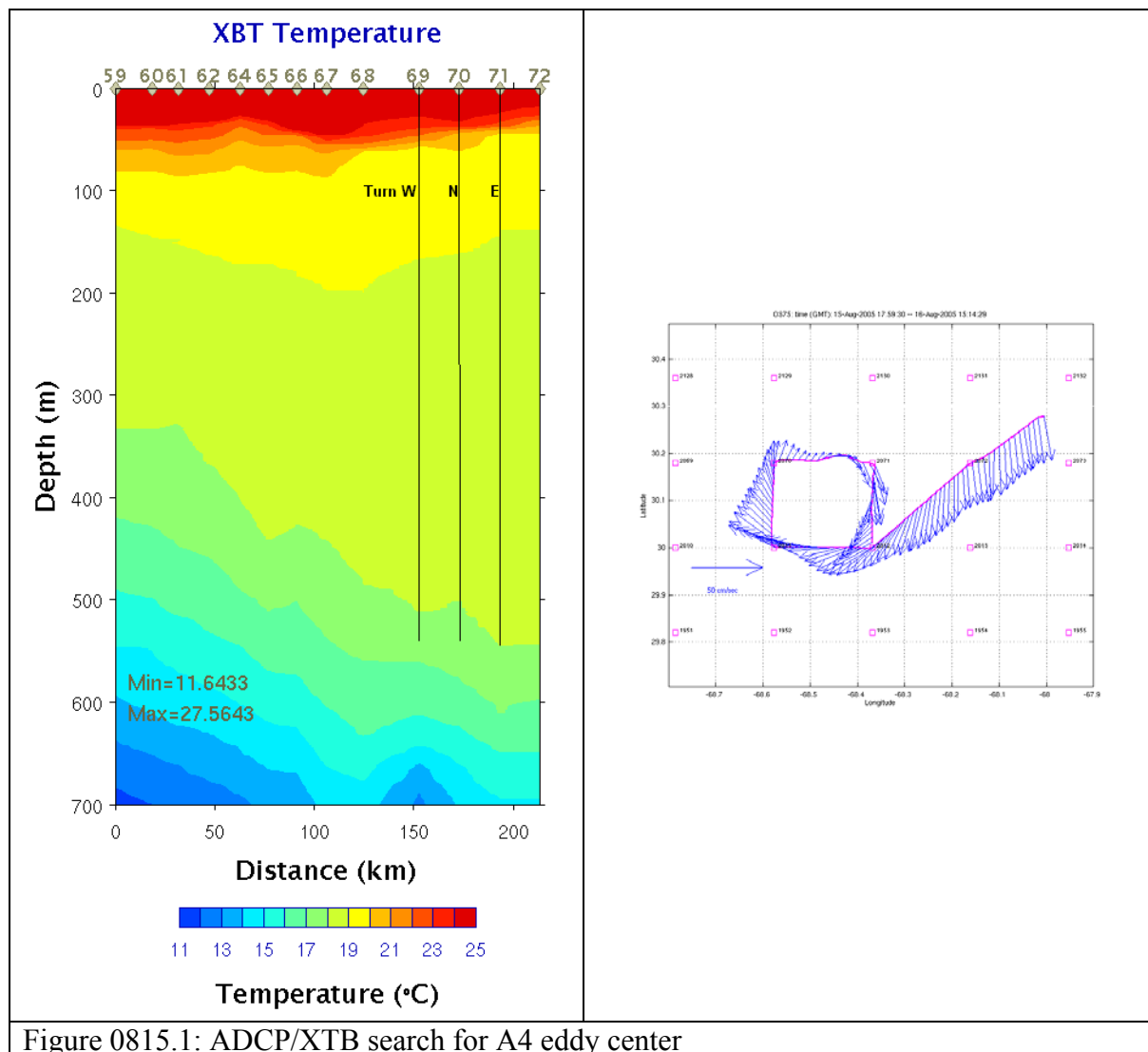


Figure 0815.1: ADCP/XTB search for A4 eddy center

August 16

VPR recovered at ca. 0300 due to data dropout. Oil in connector apparently seeped through bulkhead connector (o-ring was fine). VPR redeployed and survey continues.

August 17

VPR survey of A4 continues.

August 18

VPR survey completed, revealing a band of high fluorescence encircling eddy center in the SW, S, E, and NE quadrants (Figure 0818.1). The area of high fluorescence appears to be about half the size if was during Survey 1 (c.f. Figure 0714.1, OC415-1 cruise report). The salinity field contains mesoscale and submesoscale structure, with a complex fresh water lens in the upper ocean. Maximum salinity anomaly in the lens consists of a 0.3 ppt freshening of the upper 40m, which would amount to 32cm of rain—quite possible given recent passage of hurricane Irene. View of the density structure from the north indicates clear doming of the seasonal pycnocline at eddy center (Figure 0818.2).

Upon completion of the survey grid (see endpoint in SE quadrant of maps in Figure 0818.1), we decided to revisit the patch of high fluorescence SW of EC to determine its suitability for a deployment site for production and sediment trap arrays by WBII. Northwestward transit through the feature showed it was no longer present in that location (Figure 0818.3). Suspecting that it had been advected with the clockwise motion of the eddy, we continued northwestward and intersected it. Occupation of a partial “bowtie” pattern revealed its spatial structure, with a precipitous change in depth from its shallowest point of 70m at WP 2070, to approximately 100m 10km west and 10 km southwest of WP 2070 where fluorescence values peaked at ca. 1.8 RFU.

Joint cast with WBII at WP 2070. Small boat transfer and science meeting. CTD cast at high fluorescence patch SW of EC yields peak of $3.8 \mu\text{g l}^{-1}$ on CTD fluorometer. MOCNESS tow @ EC. Began N-S CTD transect.

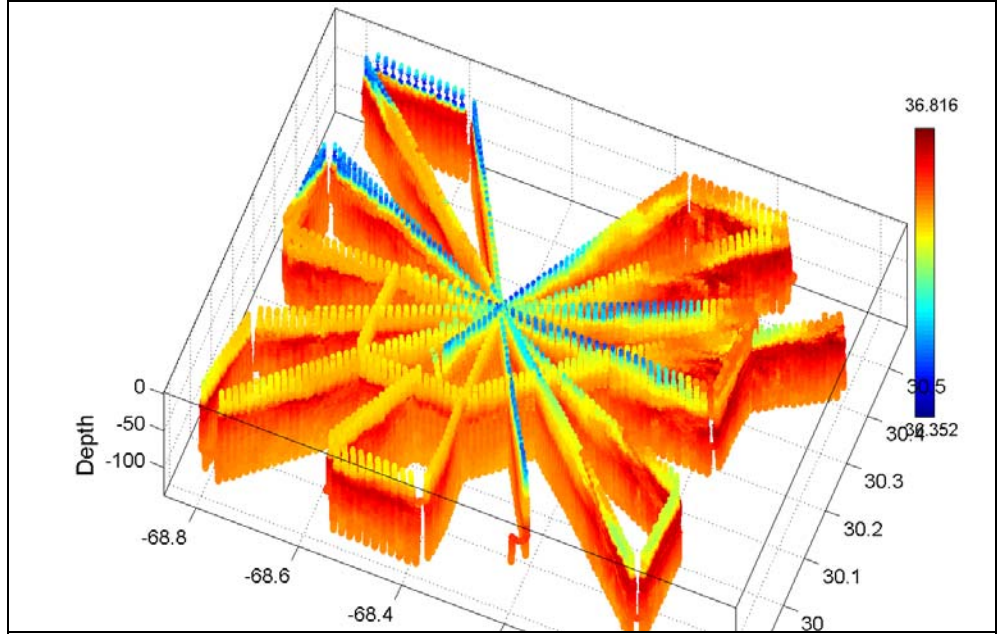
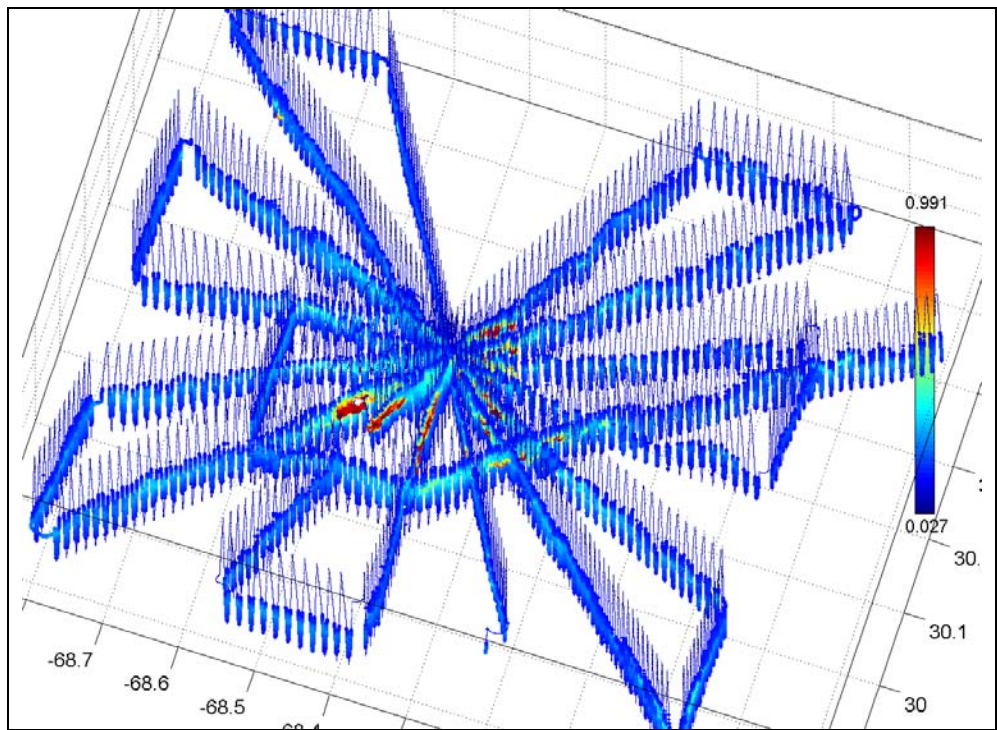
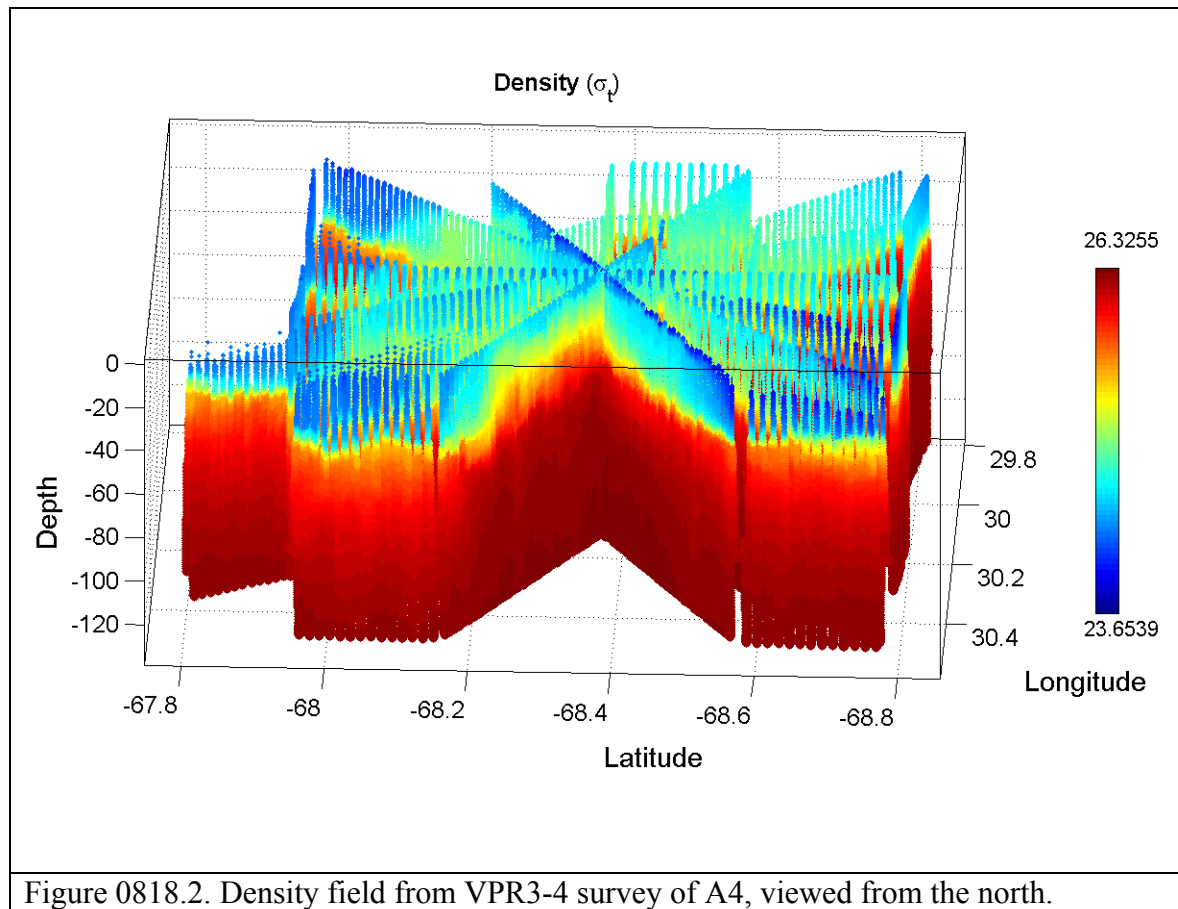


Figure 0818.1. VPR3-4 survey of A4, viewed from the southeast. Top: fluorescence; bottom: salinity. Note fluorescence scale is truncated at 1.0 RFU.



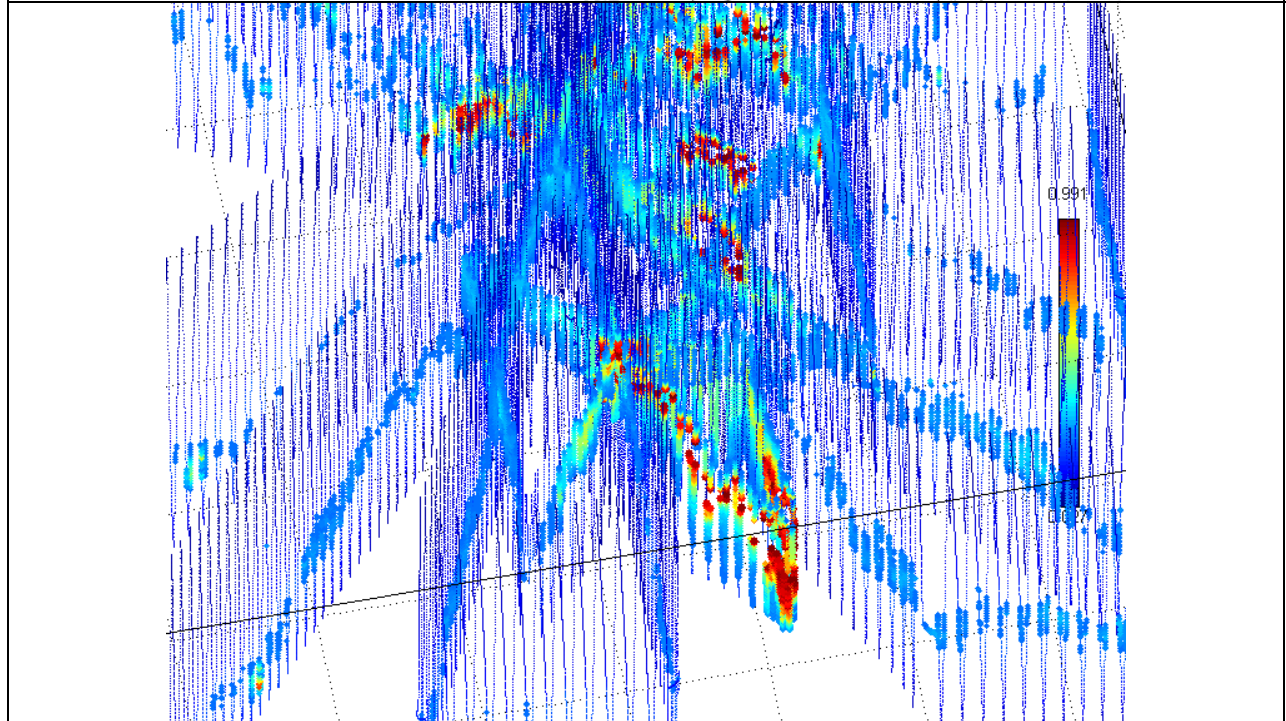
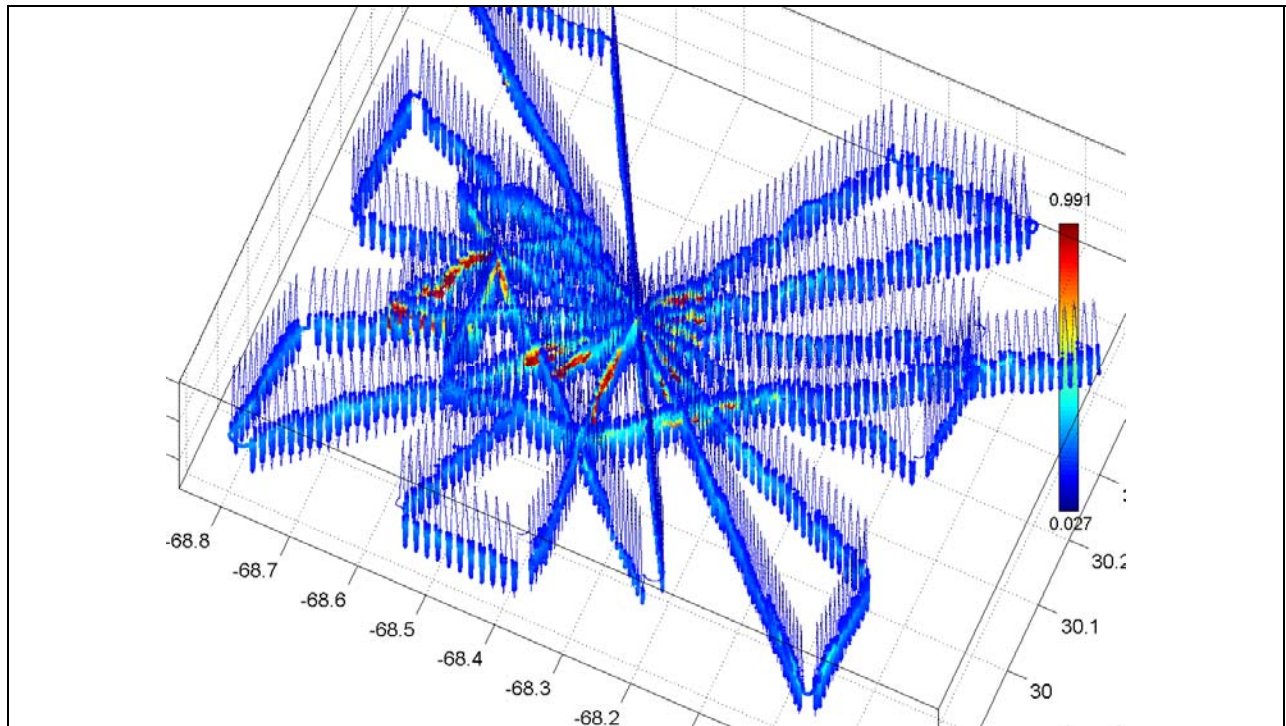


Figure 0818.3. Top: Fluorescence from VPR3-4 survey of A4 (including additional search track), viewed from the southeast. Bottom: zoom in on high fluorescence patch SW of WP 2070. Note fluorescence scale is truncated at 1.0 RFU.

August 19

N-S CTD transect continues. Daytime MOCNESS at EC.

August 20

N-S section completed, NE-SW section begun.

Day MOCNESS at NE corner.

Night MOCNESS at EC.

August 21

Day MOCNESS at SW corner.

NE-SW section completed.

E-W section begun.

August 22

E-W section completed. Fluorescence values through EC are low, ADCP data indicates SW shift of EC. Similar findings on WBII. Decided to return to EC, deploy VPR, and attempt to relocate high fluorescence patch.

August 23

VPR/ADCP survey reveals eddy center now located at WP 2010 (Figure 0823.1). A band of high fluorescence running SE-NW is located just south of eddy center (Figure 0823.2). The VPR survey was completed within 0.5 nm of WBII's sediment trap "A" just north of WP 1950. Fluorescence at that station is not particularly strong, but it is shoaled to ca. 70m (Figure 0823.2, lower right).

Drew incubation water near Sediment trap "A" and PP array; MOCNESS tow shortly thereafter. CTD cast reveals extraordinary O₂ deficit in 800-1100 m depth interval, with O₂ concentrations as low as 120 $\mu\text{mol kg}^{-1}$. [TS anomaly] Just because there is a T-S anomaly does not mean that the oxygen signal is non-local.

Transit to SE corner of the grid (1778) for CTD followed by MOCNESS tow.

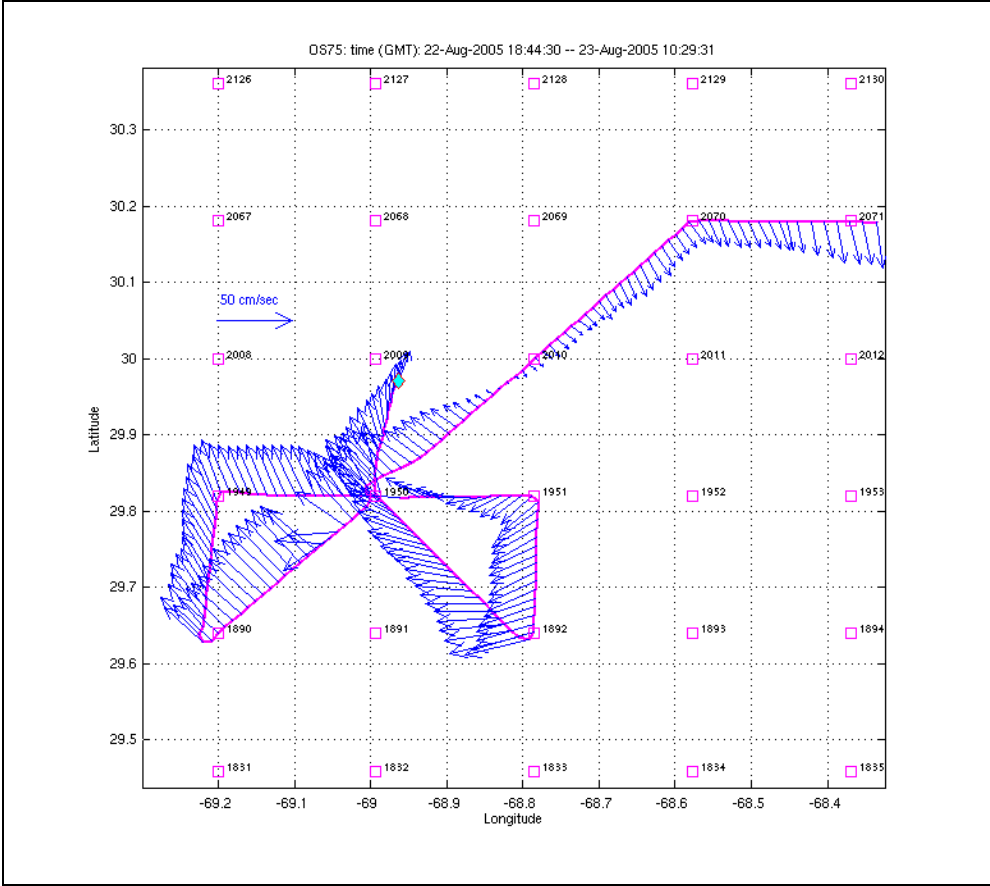
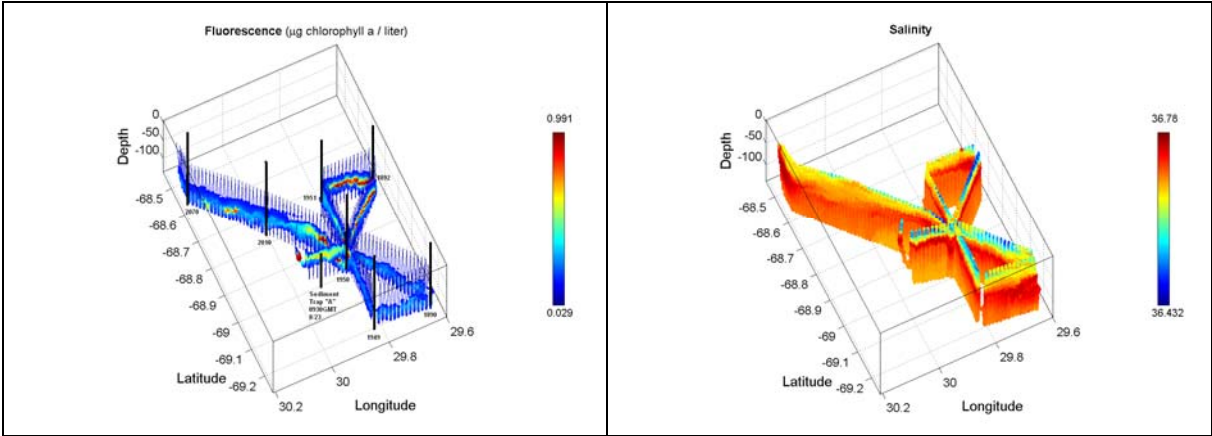
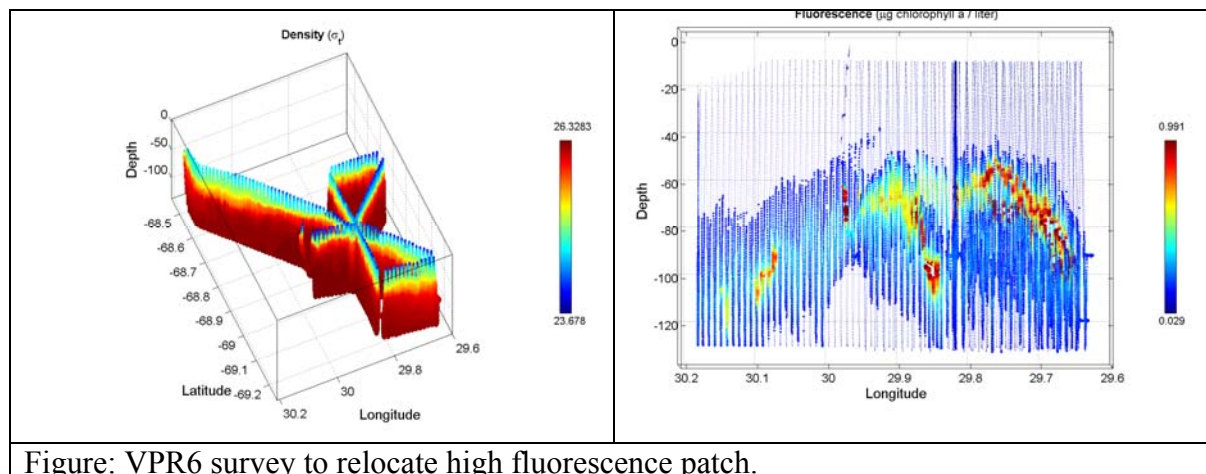


Figure 0823.1: ADCP observations during VPR6.





August 24

SE-NW transect continues.

WP 2010
 DIC sampled at 700
 Full suite at 850
 126@850

Search for EC drifter deployment location (Figure 0824.1); deployed at 1600Z 30 22.1 69 6.9, SE of 2009.

Dual cast at Sed Trap A (deep O₂ anomaly); regular sampling 0-700 plus 100m resolution of O₂, DIC, nutrients, and POC in 500-1200 depth interval.

Incubation cast (Duller) at 2184.

MOCNESS at 2184 (outside night).

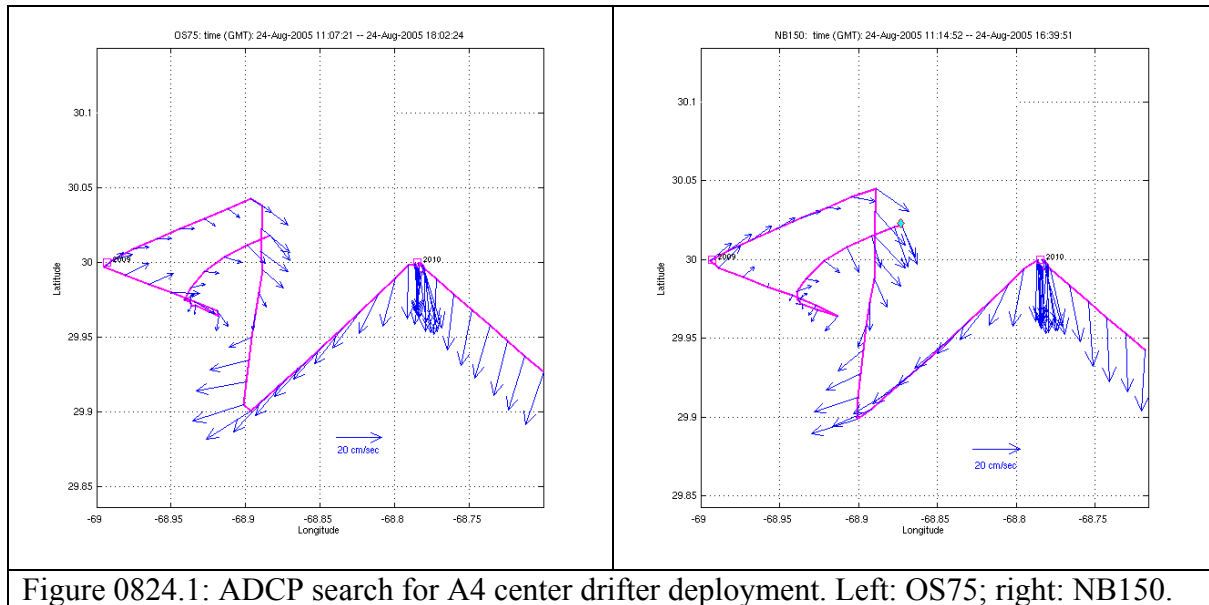


Figure 0824.1: ADCP search for A4 center drifter deployment. Left: OS75; right: NB150.

Cast at Sed trap A 1643Z 30 01 / 68 52. F=2.0 @ 130m; O₂ = 124 @ 900.

August 25

Finished NW – SE transect. Re-occupied Sed trap A 1110Z 29 56.2 / 68 49.6 for tritium samples. O₂ = 124 @ 900.

Station at 2070 to delimit NE corner of oxygen anomaly.

Begin transit to BDA.

August 26

Arrival in BDA.

3. Summary of VPR deployments, MOCNESS tows, and incubations

VPR deployments

VPR1 – 8/8 A4 core survey.
VPR2 – 8/9 continuation of A4 core survey
VPR3 – 8/12 A5
VPR4 – 8/15 transit to A4
VPR6 – 8/22 A4 core survey

MOCNESS tows

8/9/05 EC day
8/9/05 EC night
8/10/05 EC (S3) night
8/13/05 A5 EC night
8/18/05 A4 EC night
8/19/05 A4 EC day
8/20/05 A4 NE periphery (2310) day
8/20/05 A4 EC night
8/21/05 A4 SW periphery (1830) day
8/23/05 A4 Sed Trap A / PP array inside day
8/23/05 A4 SE corner (1778) night
8/24/05 A4 NW corner (2184) night

Incubations

8/9/05 EC
8/10/05 EC (S3)
8/18/05 EC (2070)
8/21/05 EC (2070)
8/23/05 Sed/PP array (ca. 1950)
8/24/05 St. 2184 Outside (Duller)

Horne calibrations

8/20/05
8/25/05

4. Comparison of CTD oxygen sensors with Winkler titrations

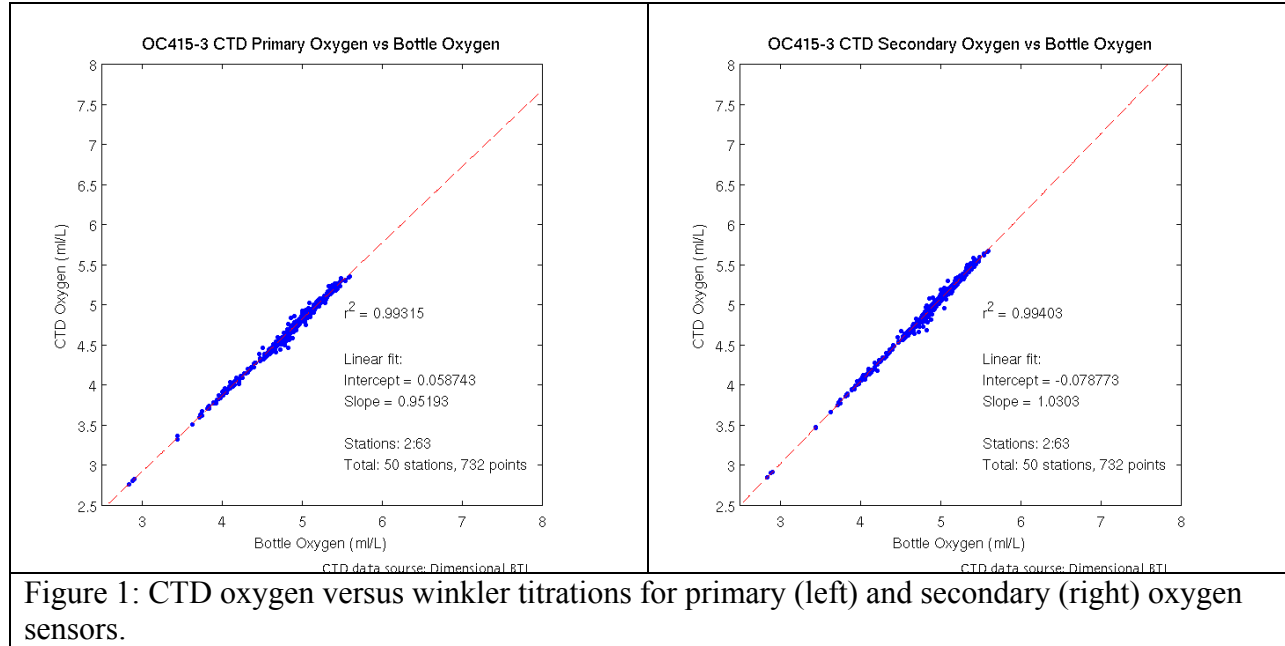


Figure 1: CTD oxygen versus winkler titrations for primary (left) and secondary (right) oxygen sensors.

5. Comparison of CTD fluorescence with extracted pigments

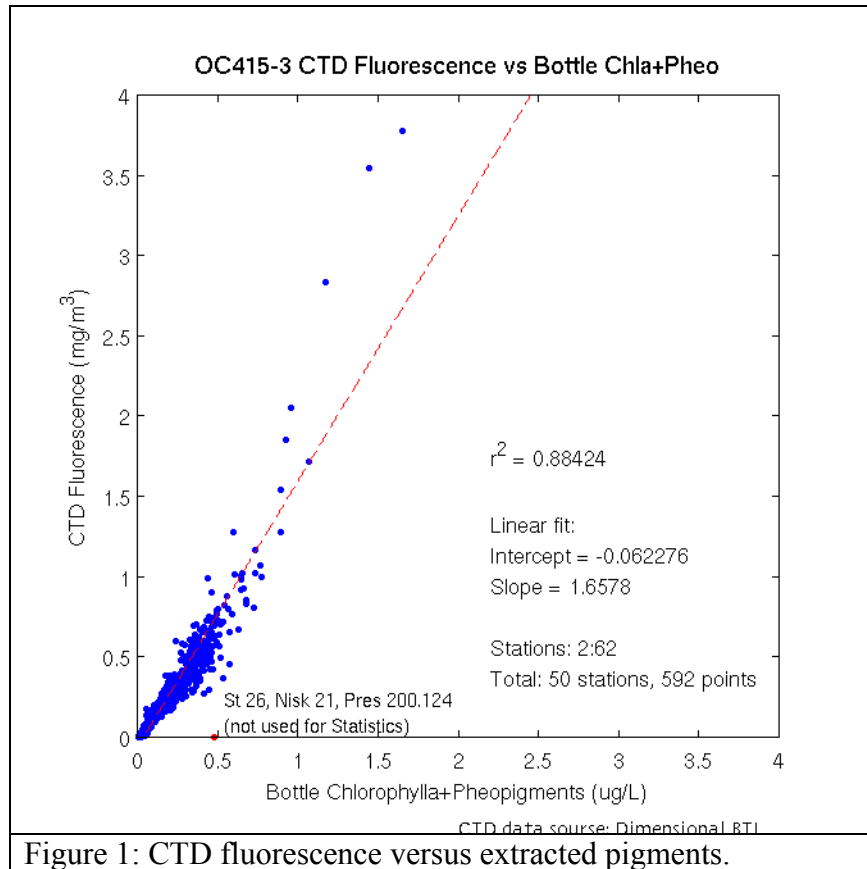
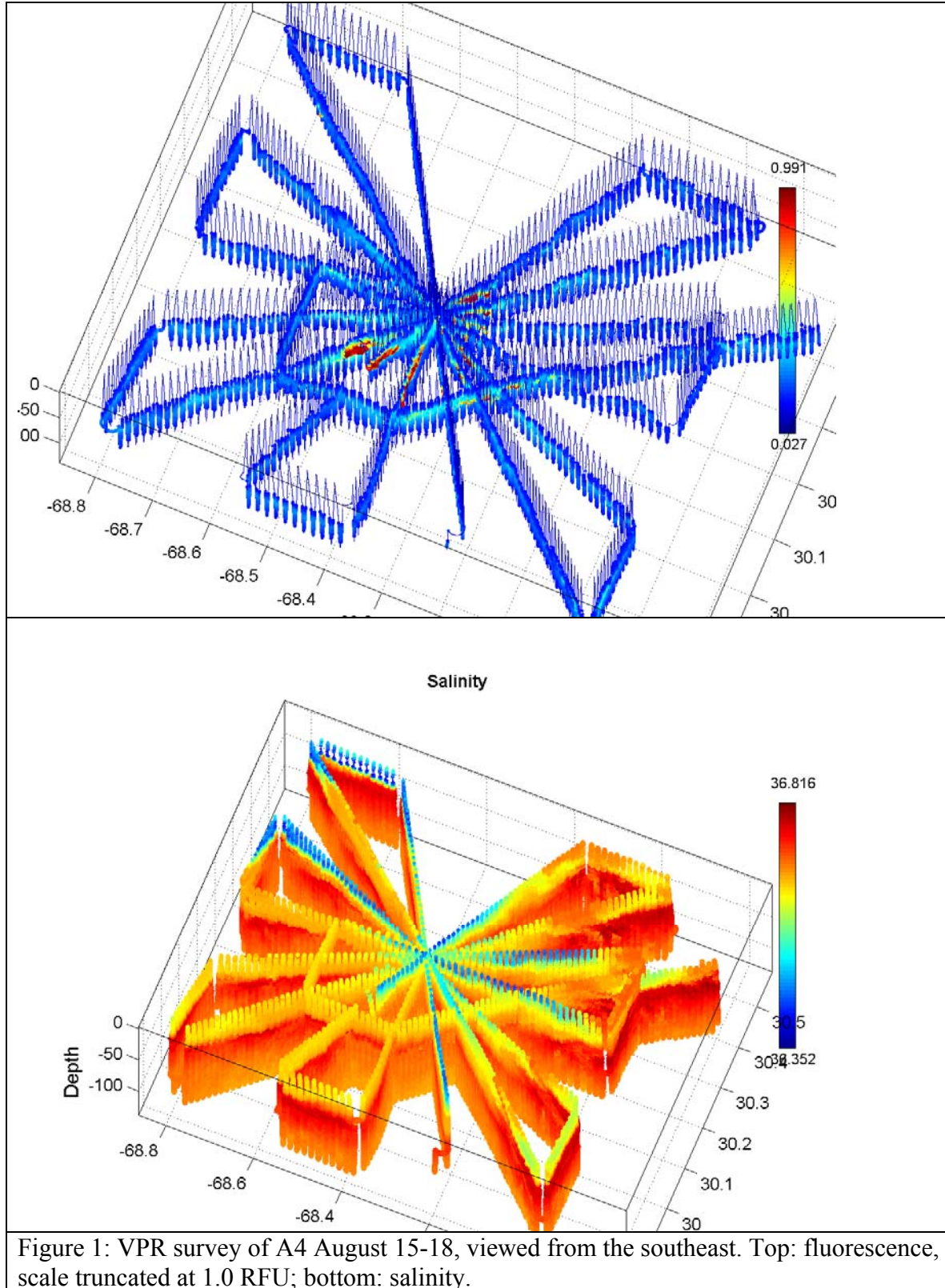


Figure 1: CTD fluorescence versus extracted pigments.

6. VPR Survey of A4



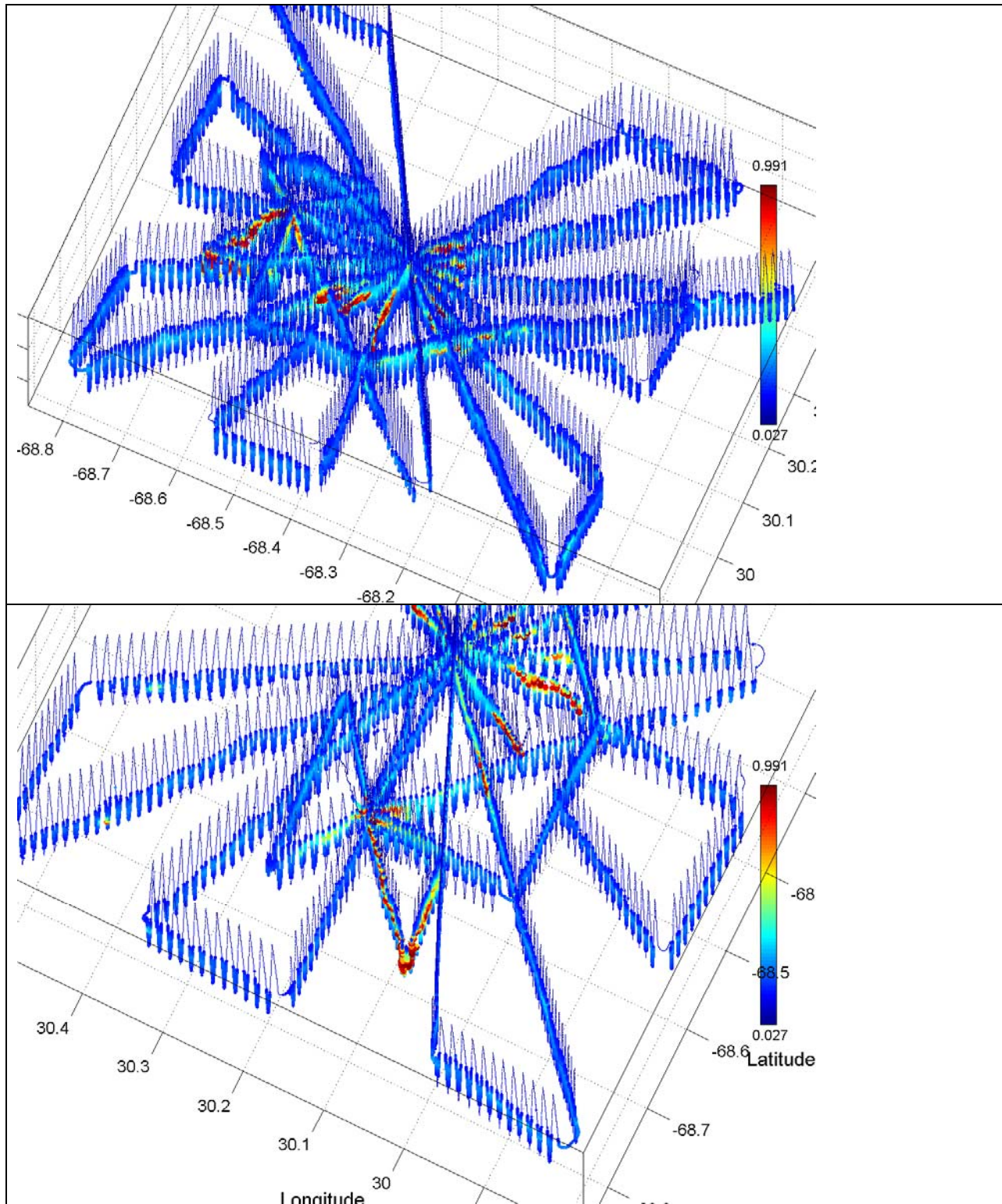


Figure 2: VPR survey of A4 August 15-18, plus addendum August 18. Top: fluorescence viewed from the southeast, scale truncated at 1.0 RFU; bottom: zoomed in view of top panel viewed from the southwest.

Diurnal variations in heat flux make clear contributions to upper ocean density structure (Figure 3). Note that areas of high stratification in near-surface waters (e.g. NW and SE corners of the survey grid) correspond to times of solar heat input; lower stratification areas are associated with night-time VPR transits. A temporal trend over the length of the survey is also evident.

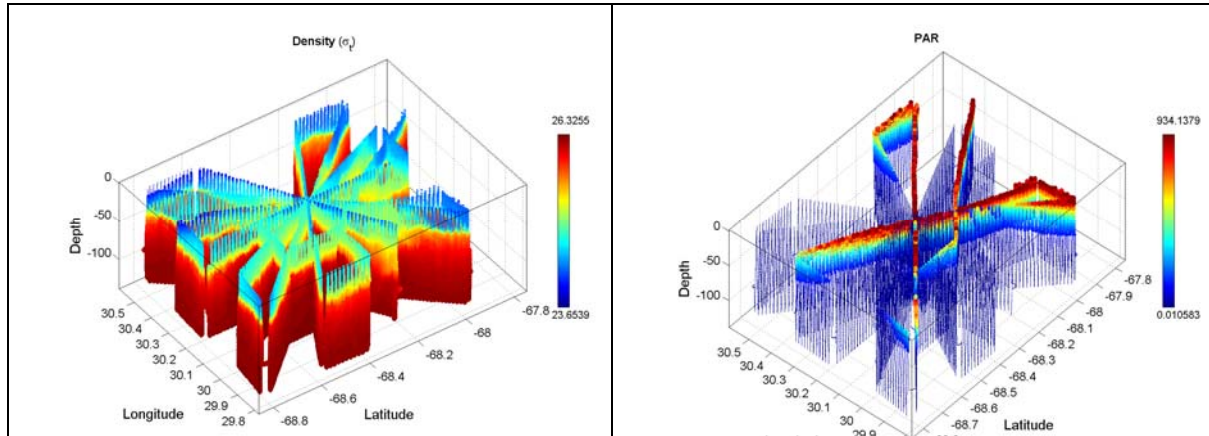


Figure 3: Density (left) and PAR (right) for VPR survey of A4, viewed from the SW.

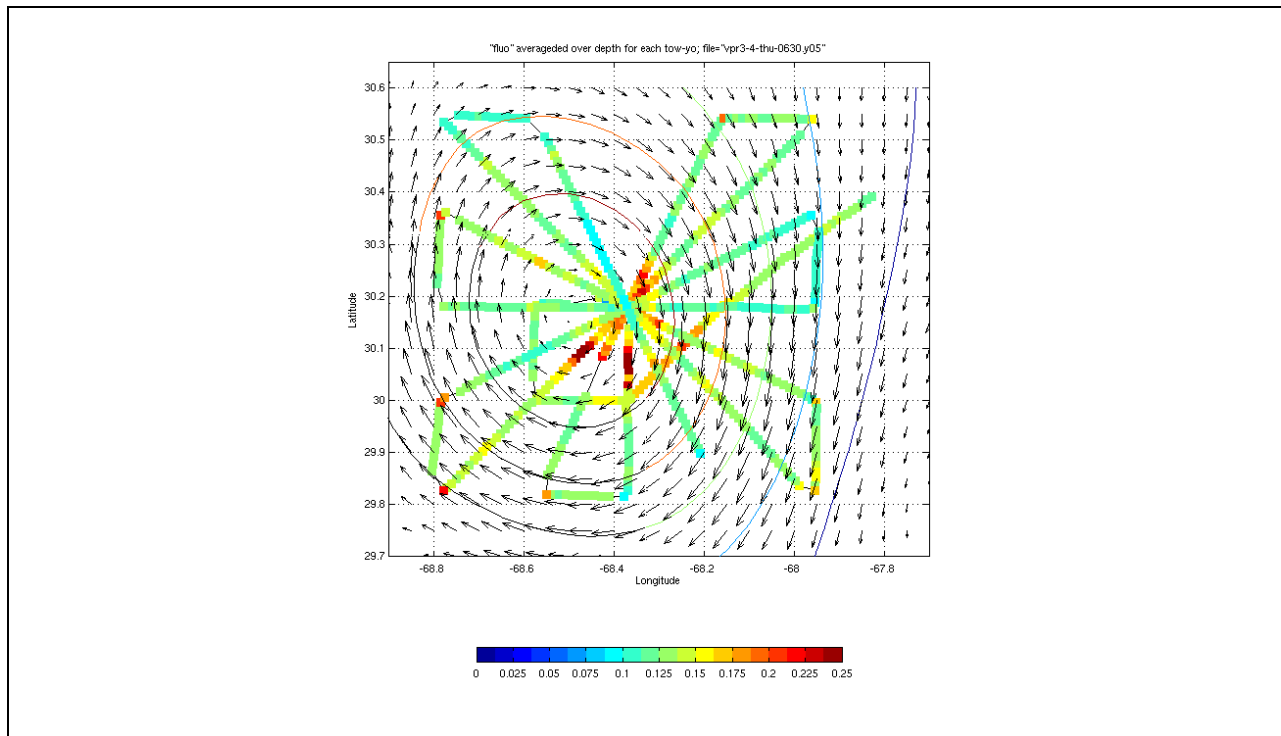


Figure 4: Fluorescence averaged over each towyo of A4 VPR survey. Note that turning points yield longer towyos, resulting in higher than average fluorescence. In all other areas, towyos are of equal length and therefore the map can be interpreted as a vertical average. An optimal interpolation of ADCP current velocities is superimposed.

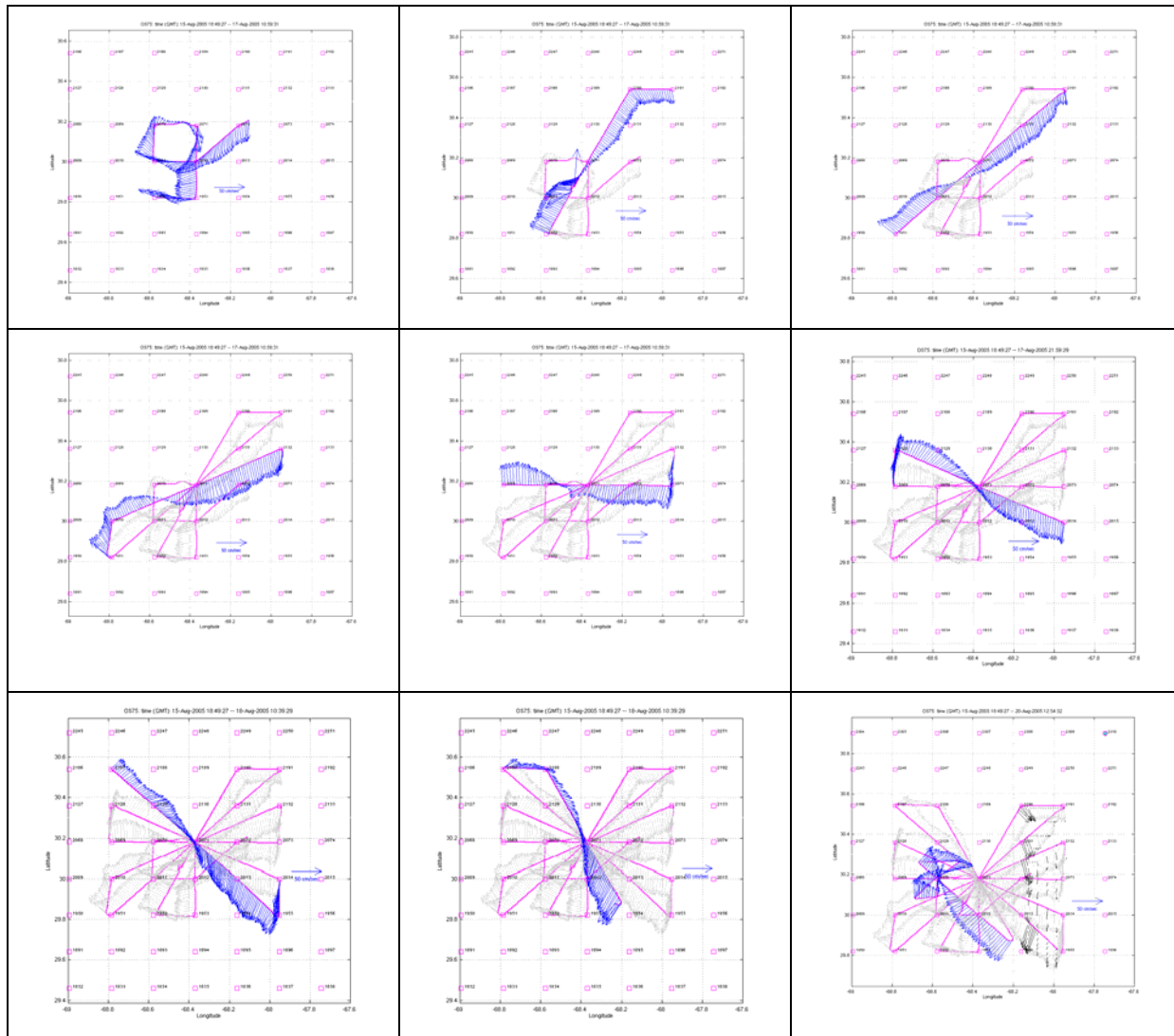


Figure 5: ADCP velocities during A4 VPR survey.

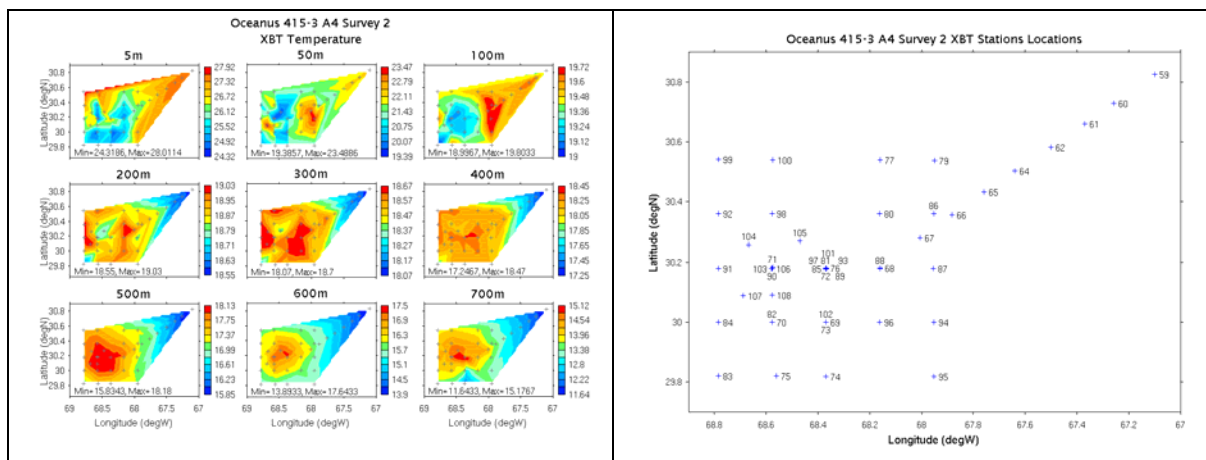


Figure 6: XBT temperatures observed during A4 VPR survey.

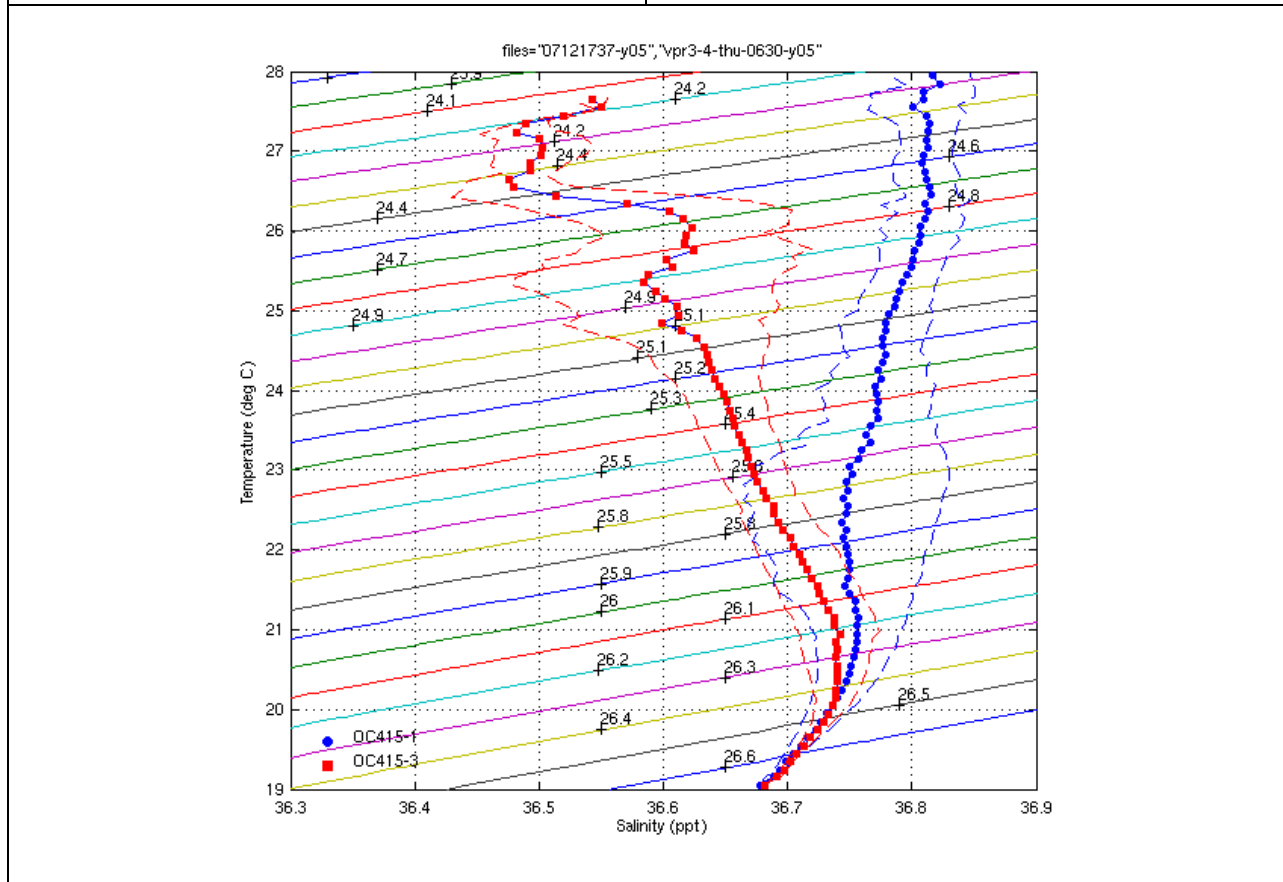
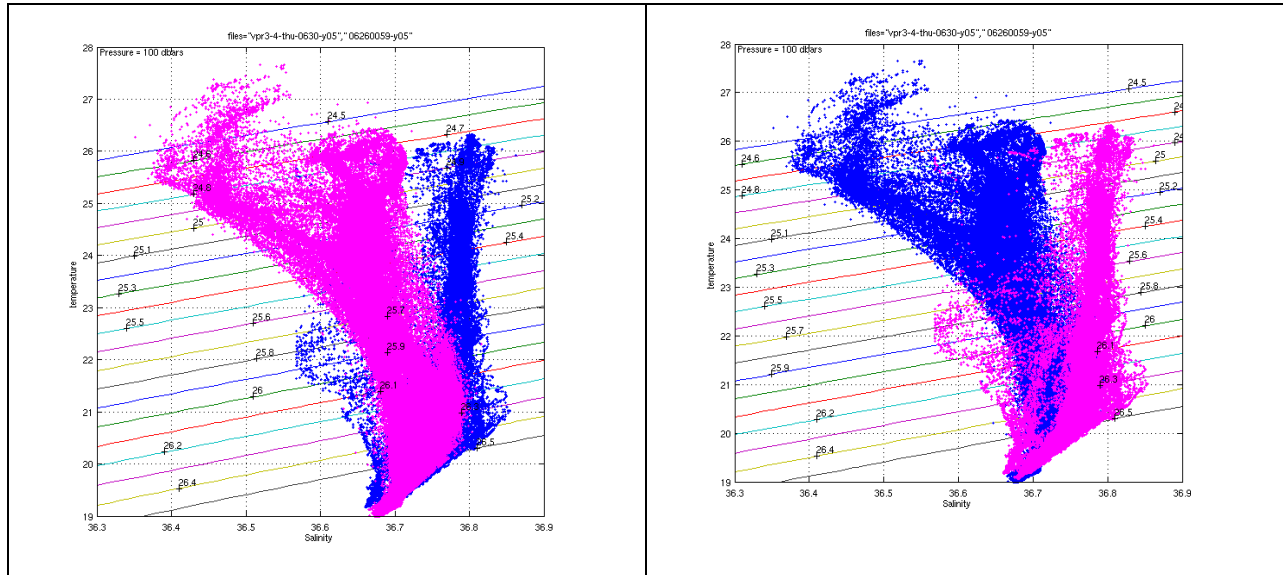


Figure 7: T-S diagrams for VPR surveys of A4 during OC415-1 and OC415-3. Color schemes in upper panels are reversed left and right for comparison. Upper left: OC415-1 blue, OC415-3 pink; upper right: OC415-1 pink, OC415-3 blue. Lower panel: mean values and standard deviations.

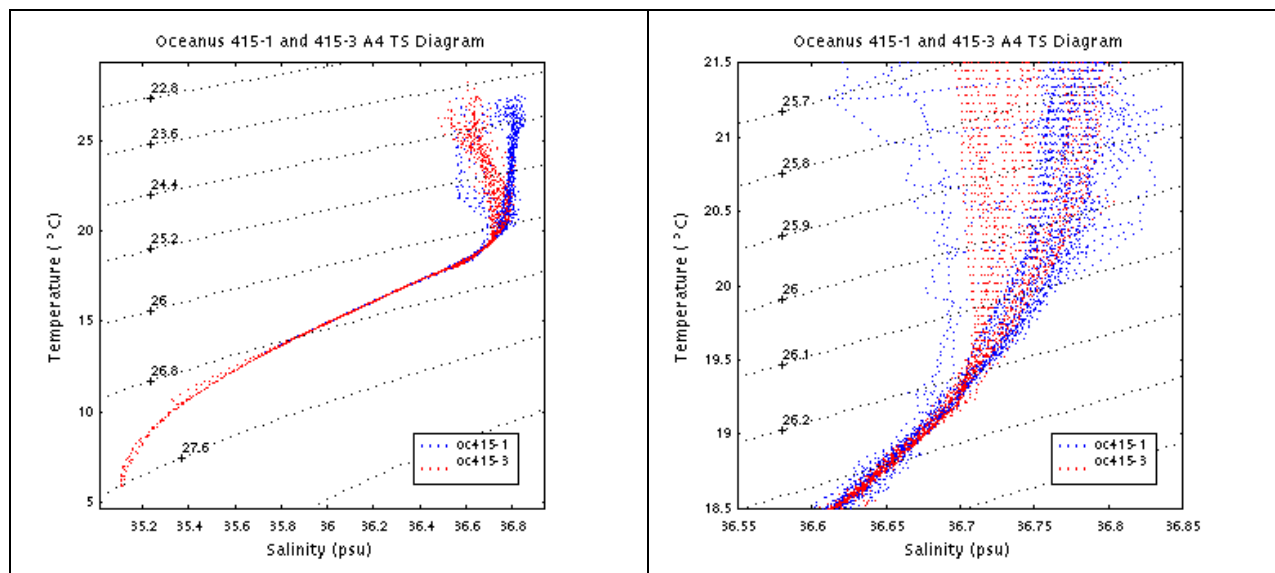


Figure 8: TS diagrams from OC415-1 and OC415-3 surveys of A4 over the full range of observations (left) and zoomed in on the upper ocean (right). Note that the 1200m casts carried out in OC415-3 span a wider range of T and S than the 700m casts of OC415-1 (left).

Comparison of T-S characteristics for VPR surveys of A4 during OC415-1 and OC415-3 reveals the signature of seasonal heating and freshwater input at the surface due to storm activity (Figure 7). However, there does not appear to be any discernible warming in the 26.2 to 26.3 density range—if anything it appears that waters of those densities have gotten slightly colder and fresher over time, presumably due to mixing.

T-S characteristics from the CTD data confirm the second survey of A4 is in the same water mass (Figure 8, left panel). There is no sign of heating in the density range 26.2-26.3.

***note the OC415-1 “survey” is just single section across A4.

The fluorescence distribution in A4 exhibits distinctive structure in density space (Figure 9). Surveys of A4 during OC415-1 and OC415-3 both show peak fluorescence values in the neighborhood of $\sigma_T=26.25$. The scatterplots suggest broadening of the fluorescence peak over time, along with a shift toward a slightly denser isopycnal in the later cruise. However, neither of these apparent shifts are statistically significant (Figure 9, right panel).

Another salient characteristic of the fluorescence-density relationship is the secondary peak in the density range 26.0-26.2. Interestingly, fluorescence in this density range exhibits clear spatial structure, with highest values around the periphery of the eddy core (Figure 10). The band of enhanced fluorescence in the 26.0-26.2 density interval appears to covary with the salinity field, particularly in OC415-1 where the secondary maximum disappears in the relatively fresh waters in this density range present in the eddy core. These patterns suggest different phytoplankton populations are associated with these two peaks insofar as their spatial distributions are distinct. Presumably whatever environmental factor is leading to the bloom of chain-forming diatoms in the eddy core is not favorable to the organisms that comprise the secondary peak residing in the lighter isopycnals in the periphery of the core.

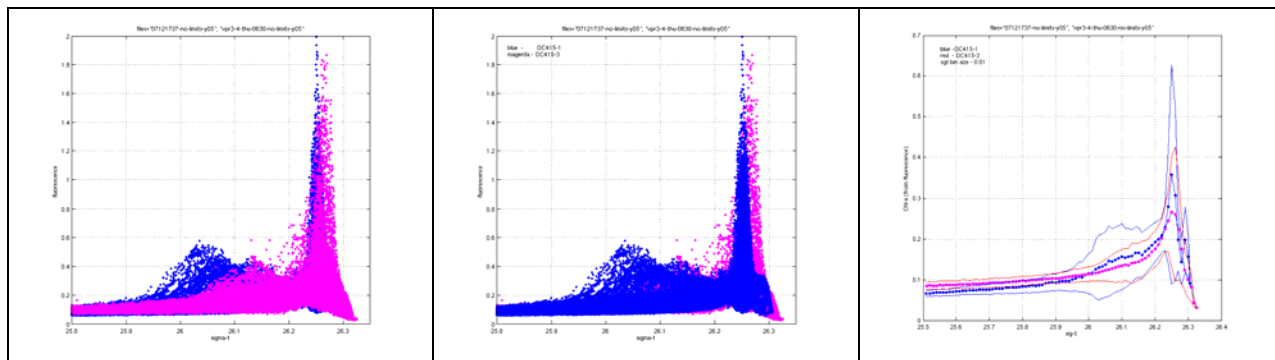


Figure 9: Distribution of fluorescence versus density for VPR surveys of A4 during OC415-1 and OC415-3. Left two panels: aggregate data, with color schemes reversed to reveal patterns. Right panel: means and standard deviations.

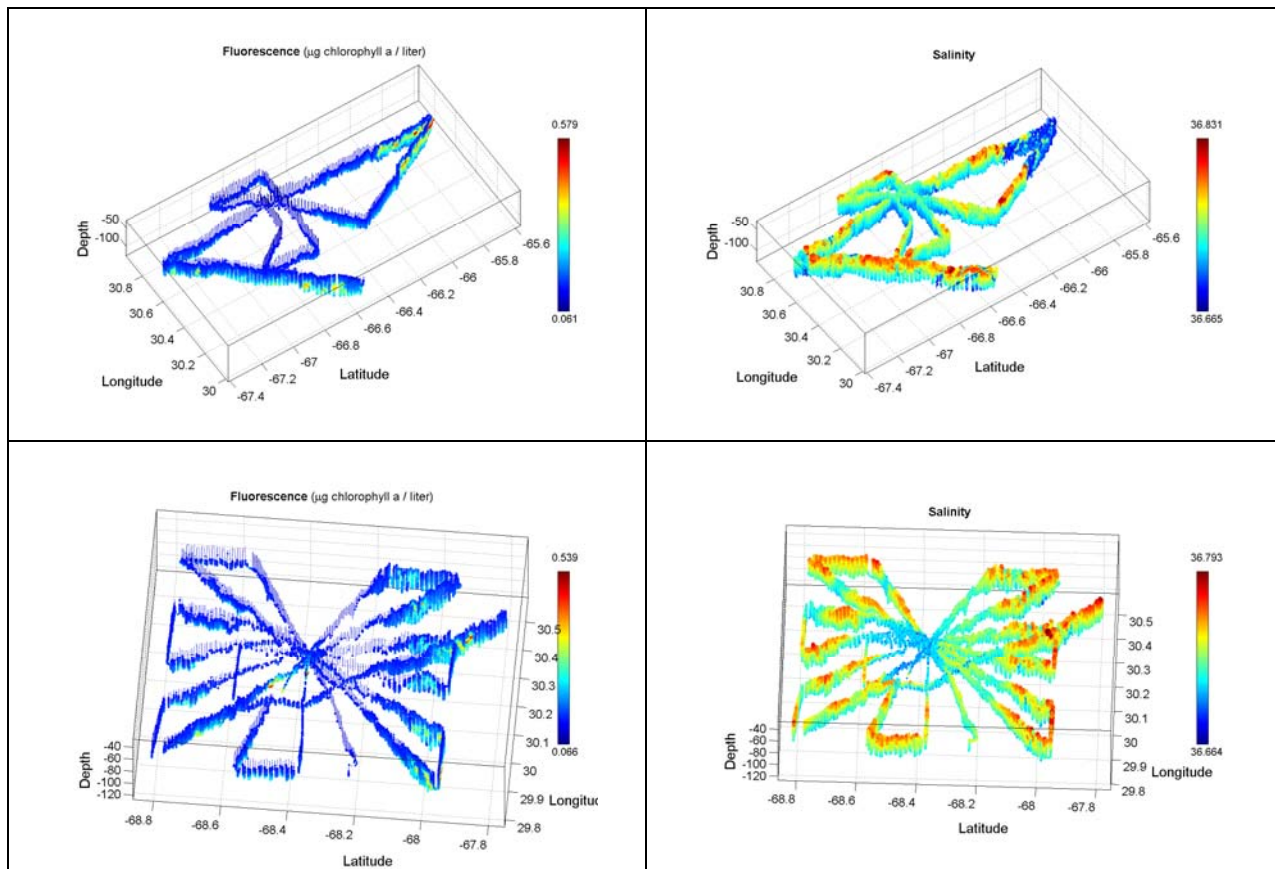


Figure 10: Distribution of fluorescence (left) and salinity (right) in the density range 26.0 to 26.2 for VPR surveys of A4 during OC415-1 (top) and OC415-3 (bottom).

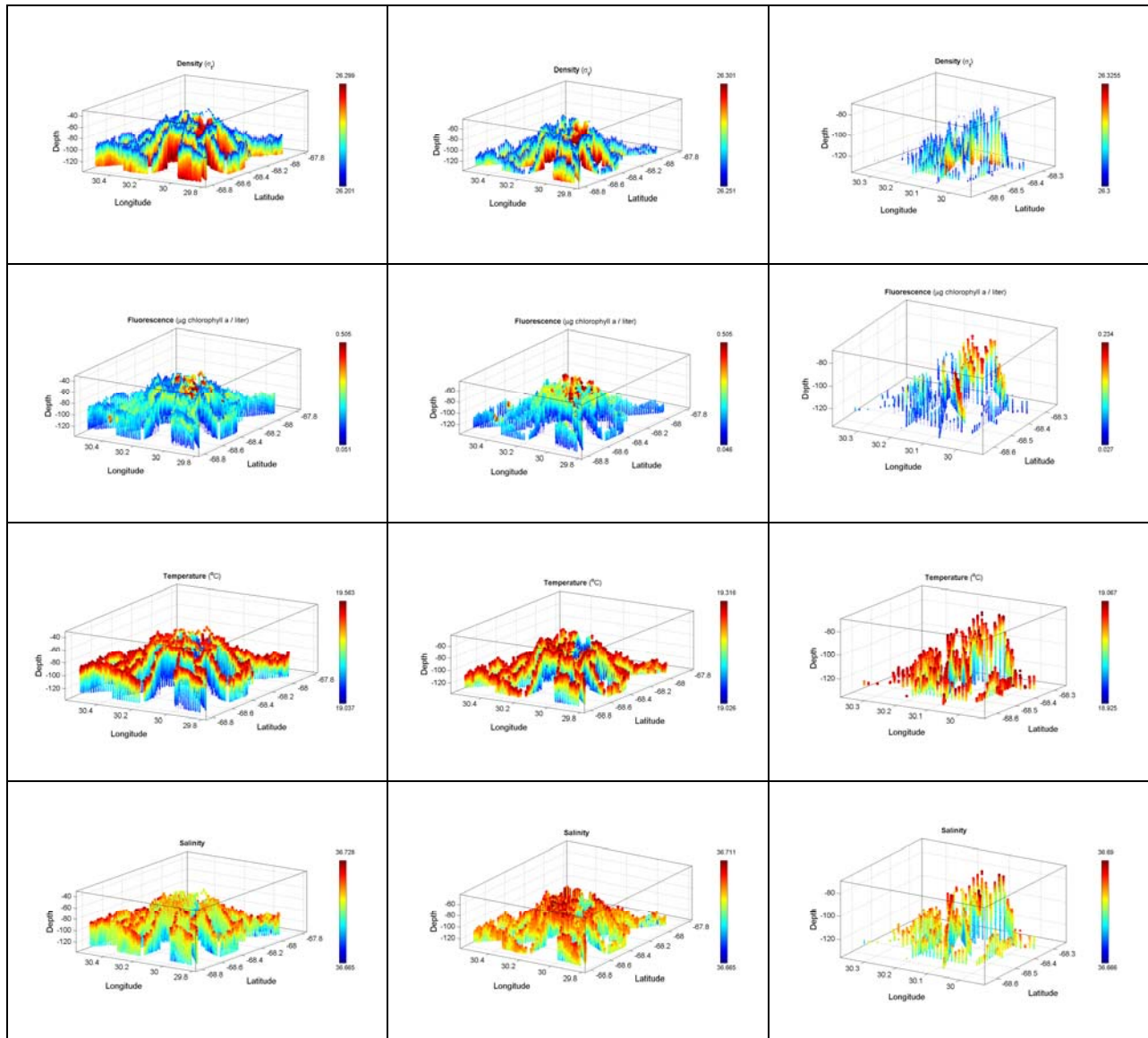


Figure 11: A4 density, fluorescence, temperature, and salinity distributions for density ranges 26.2-26.3 (left), 26.25-26.3 (middle), and 26.3-26.35 (right).

7. Diatom distributions from VPR data

Finding: the three-dimensional distribution of diatoms with respect to the fluorescence field is complex: abundance of diatoms is higher in the fluorescence maximum, but they are also present elsewhere in the water column (Figure 1). Vertically averaged fluorescence and diatom concentrations covary spatially and their correlation is highly significant (Figure 2).

A histogram of fluorescence values from the (t,x,y,z) locations of each diatom observation point (fluorescence at diatom point, or FADP) reveals that most diatoms are observed at low fluorescence values (Figure 3, upper left panel). However, the VPR spends most of its time in low-fluorescence water, as evidenced by a histogram of fluorescence values from the VPR log file (Figure 3, upper right panel). Therefore it is of interest to normalize the FADP distribution by the aggregate fluorescence (AF) distribution (Figure 3, lower panels, expressed as a fraction and also as percent of total). Peak abundances of diatoms are clearly associated with peak fluorescence concentrations ($F > 1.0 \mu\text{g l}^{-1}$), yet significant numbers of diatoms occur at lower fluorescence ($F < 1.0 \mu\text{g l}^{-1}$). Approximately 46% (54%) of the diatoms observed were present at fluorescence values less (greater) than $1.0 \mu\text{g l}^{-1}$ (Table 1).

Data from VPR4-5 generally corroborate these findings (Figures 4, 5), although the diatoms in this later time period appear to be more strongly associated with high fluorescence, with the percentage of total diatoms in the highest fluorescence bin rising from 54% to 64% (Table 1). Whether or not this change is statistically significant is difficult to determine, as spatial coverage of the two surveys is quite different: VPR1-2 consists of a few sections, whereas VPR4-5 is a more complete survey.

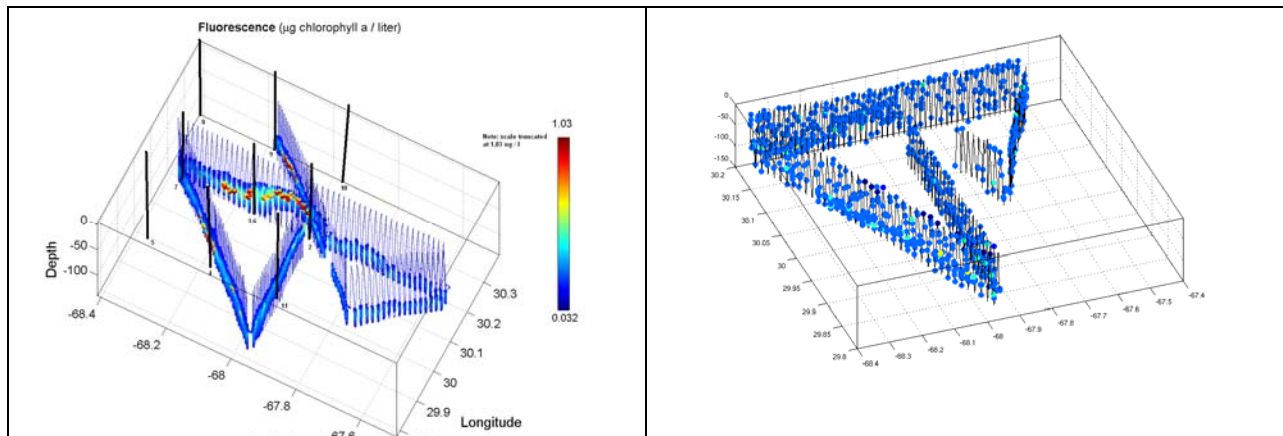


Figure 1. Fluorescence (left) and diatom concentration (right) from VPR 1 and VPR 2. Note the vantage point for fluorescence is from the SE, whereas that for diatom concentration is SW.

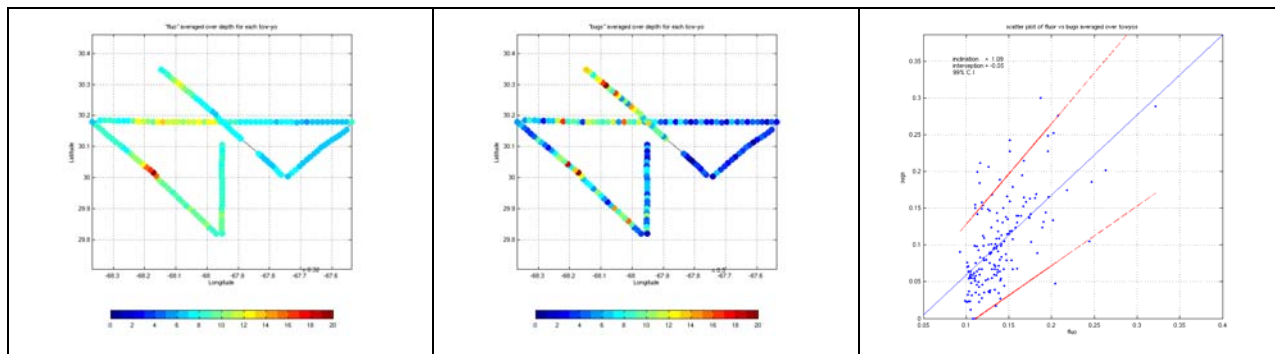


Figure 2. Vertically averaged fluorescence (left) and diatom concentration (middle) from VPR 1 and VPR 2. Right: correlation between vertically averaged fluorescence and diatom concentration.

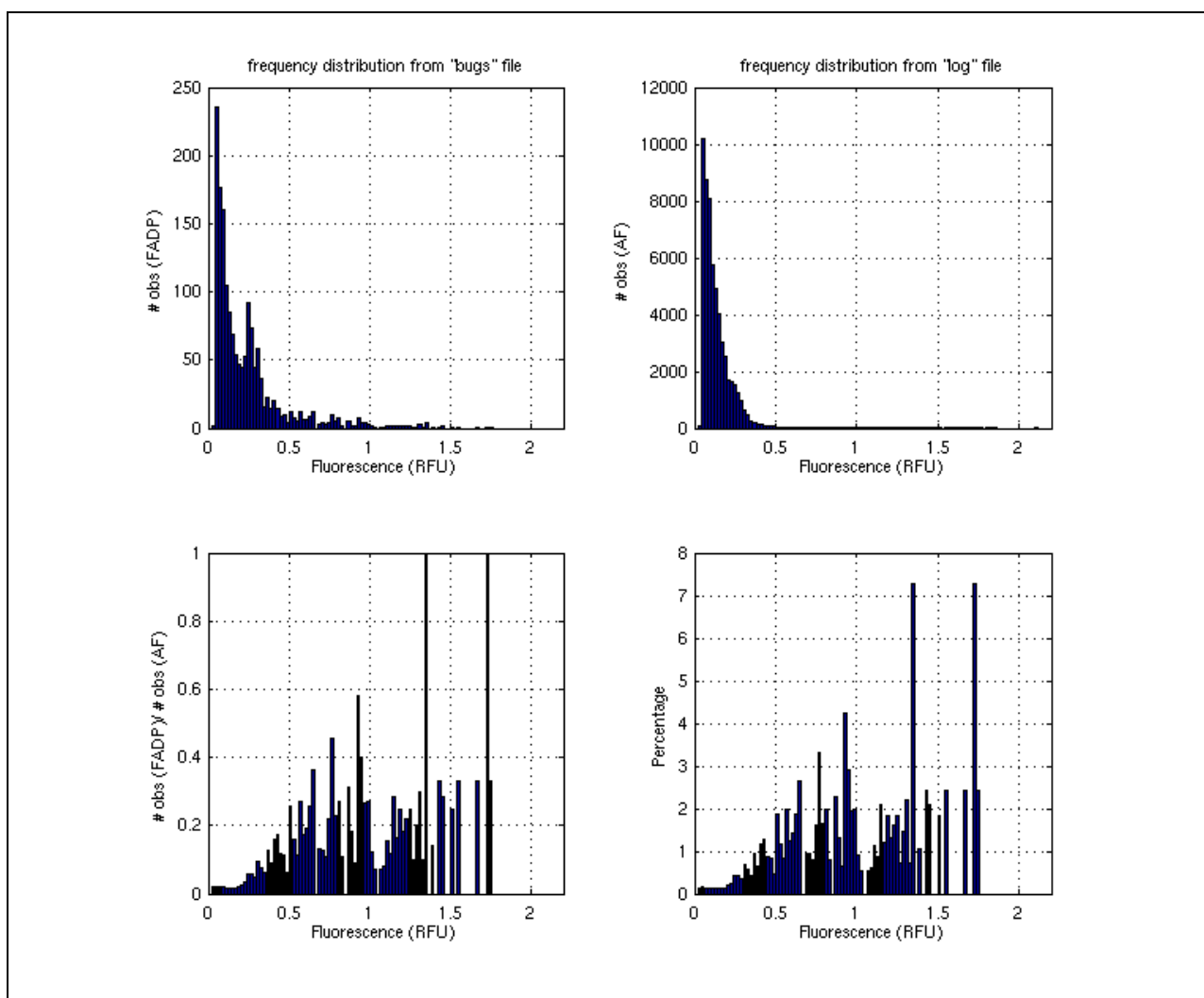


Figure 3: Binned distribution of fluorescence observations at diatom points (FADP) [upper left] and aggregate fluorescence (AF) [upper right]. Lower panels: ratio of FADP to AF distributions, expressed as both a raw fraction (left) and as a percentage of the total number of FADP observations.

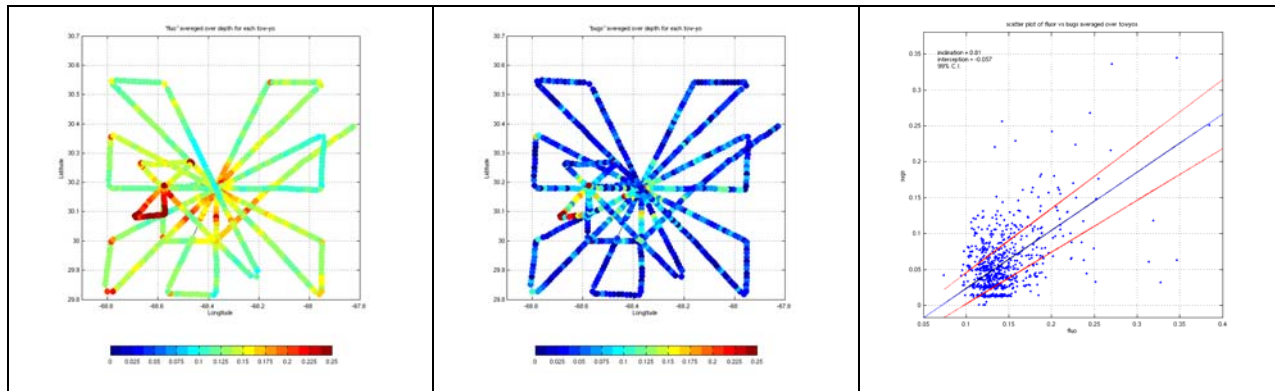


Figure 4. Vertically averaged fluorescence (left) and diatom concentration (middle) from VPR4-5. Right: correlation between vertically averaged fluorescence and diatom concentration.

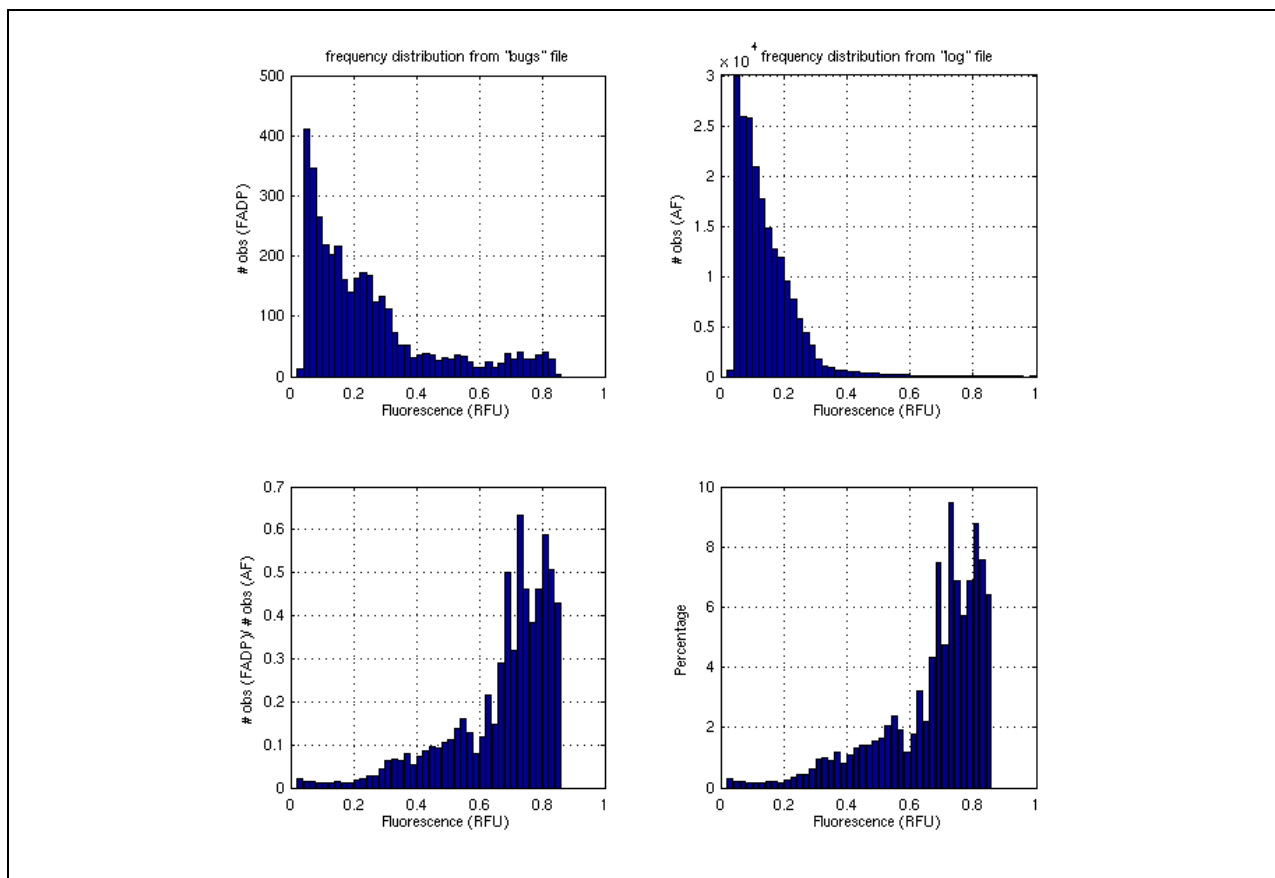


Figure 5: Binned distribution of VPR4-5 fluorescence observations at diatom points (FADF) [upper left] and aggregate fluorescence (AF) [upper right]. Lower panels: ratio of FADF to AF distributions, expressed as both a raw fraction (left) and as a percentage of the total number of FADF observations.

Table 1: Percentage of diatoms present in various fluorescence intervals.

Fluorescence bin	% of total VPR1-2	% of total VPR4-5
0.0-0.5	4.95	1.9
0.5 – 1.0	40.64	7.0
1.0 – 1.5	29.58	26.7
1.5 – 2.0	24.81	64.4

Data

Diatom locations $D_i(t,x,y,z,F)$
 Diatom concentration (from binned D_i)
 VPR log file $V_j(t,x,y,z,F)$

Sample rates

Camera: 30 frames s^{-1}
 VPR log file: 1 s^{-1}

Preprocessing

VPR 1 and VPR 2 data sets combined
 Launch and recovery periods removed from VPR log files

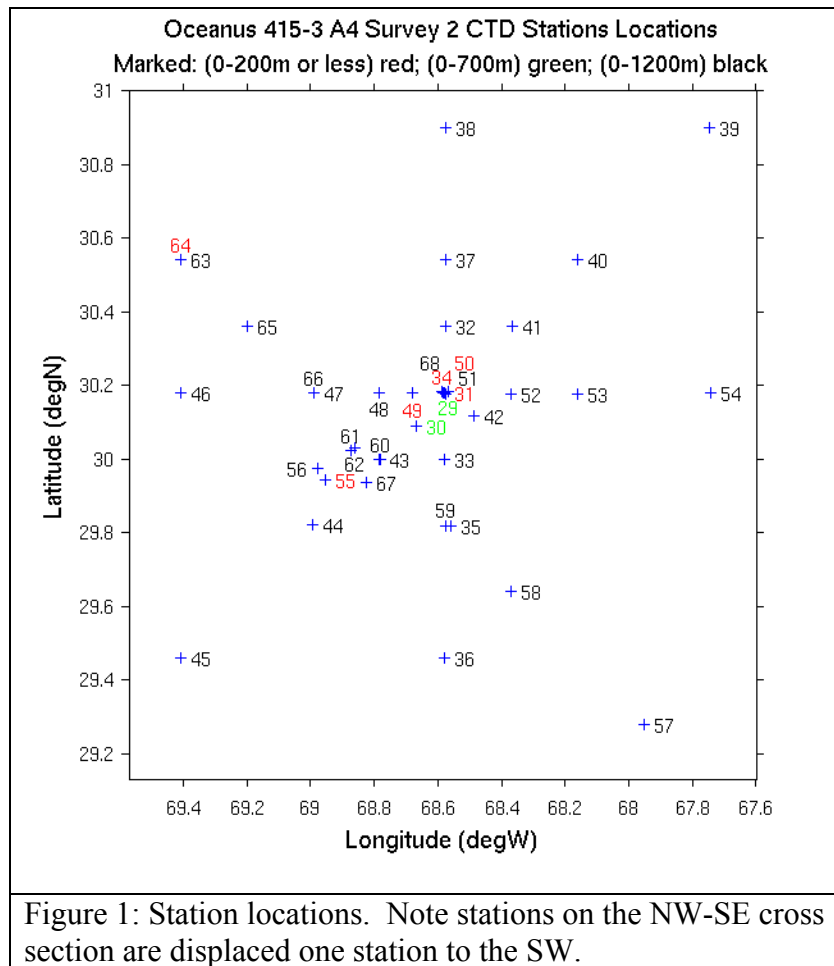
Histogram 1: (from D_i): $N_1 = \#$ of diatoms in fluorescence bins [0:.02:2.0]

Histogram 2: (from V_j): $N_2 = \#$ of fluorescence observations in fluorescence bins [0:.02:2.0]

Histogram 3: N_1 / N_2

Note that it is possible for the ratio computed in histogram 3 can exceed 1. The sample rate of the camera is a factor of 30 higher than the VPR log file, so if multiple diatoms are observed within a 1-second time interval, they will all point to the same entry in the log file.

8. Vertical sections from A4 CTD survey



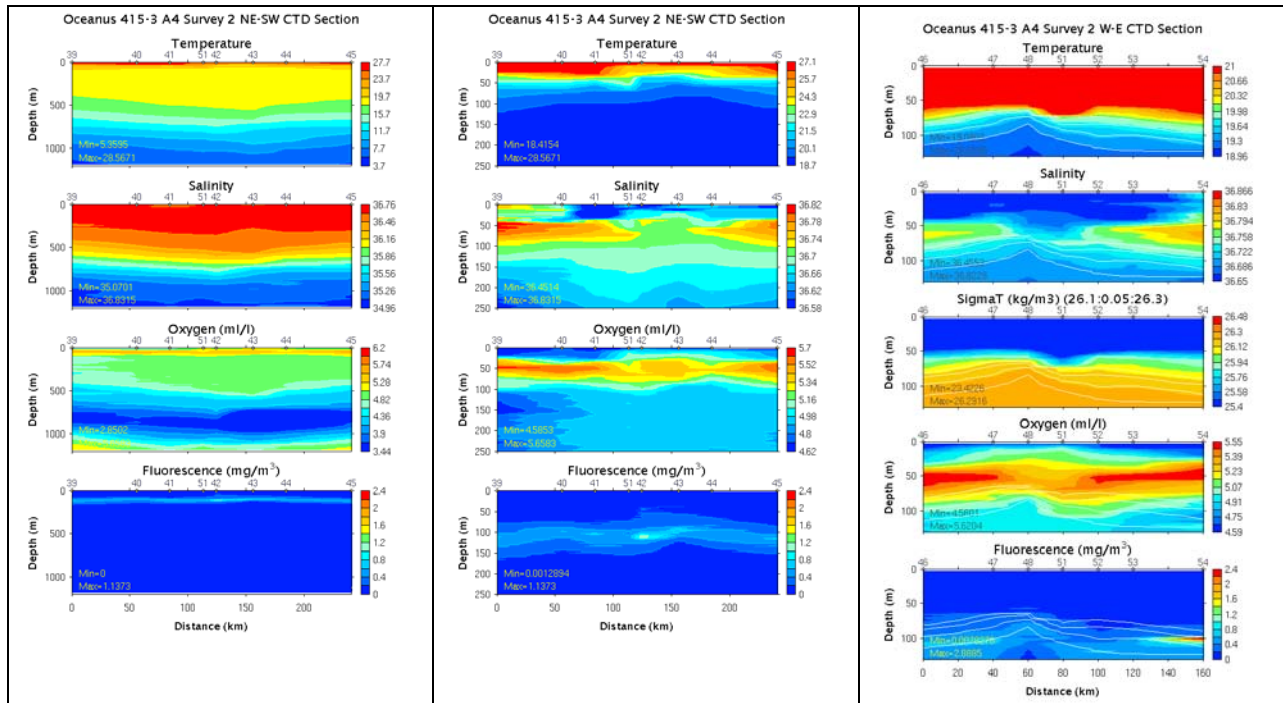


Figure 2: NE-SW Section across A4. Left: 0-1200m; middle: 0-250m; right: 0-125m. Density contours $\sigma_T = 26.1, 26.15, 26.2, 26.25, 26.3$ are shown in white on the right panel.

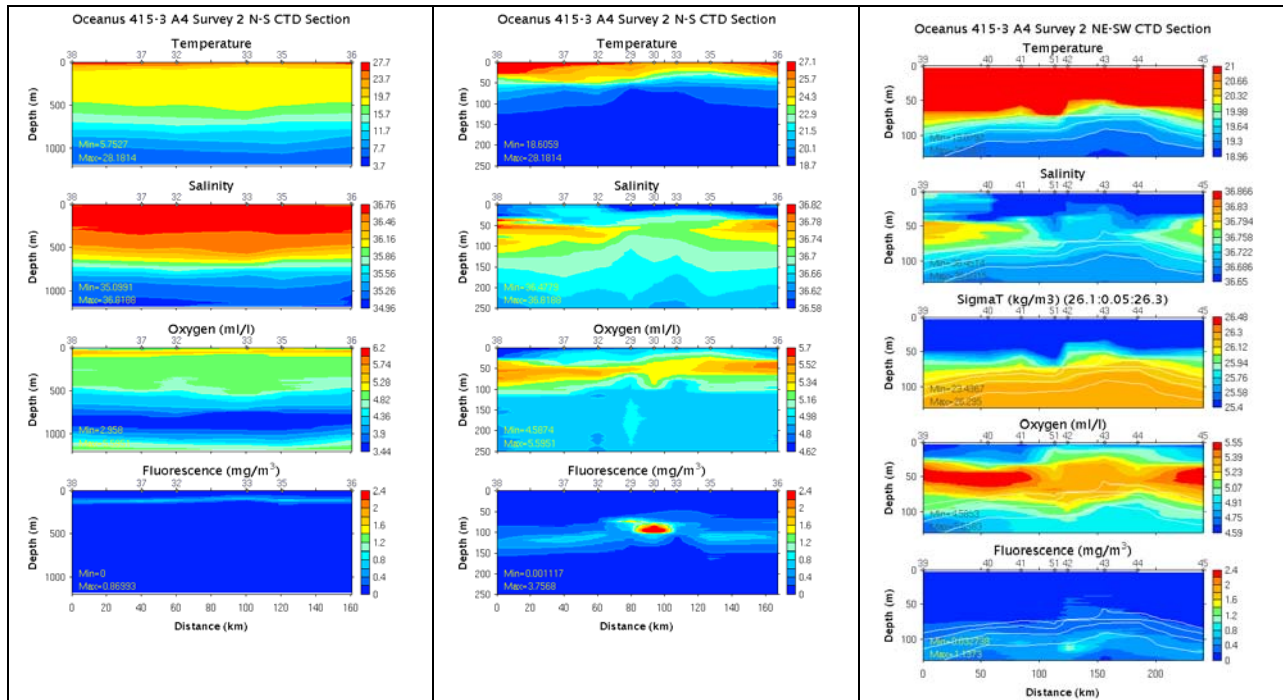


Figure 3: N-S Section across A4. Left: 0-1200m; middle: 0-250m; right: 0-125m. Density contours $\sigma_T = 26.1, 26.15, 26.2, 26.25, 26.3$ are shown in white on the right panel.

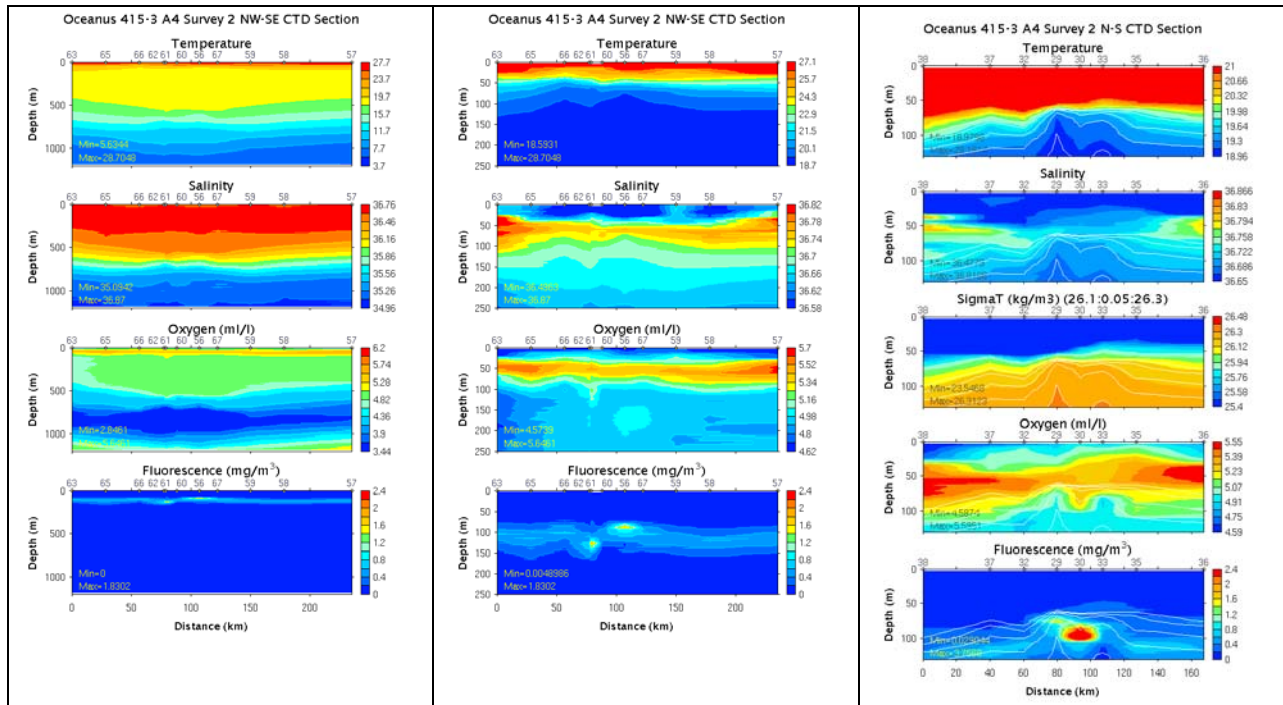


Figure 4: NW-SE Section across A4. Left: 0-1200m; middle: 0-250m; right: 0-125m. Density contours $\sigma_T = 26.1, 26.15, 26.2, 26.25, 26.3$ are shown in white on the right panel.

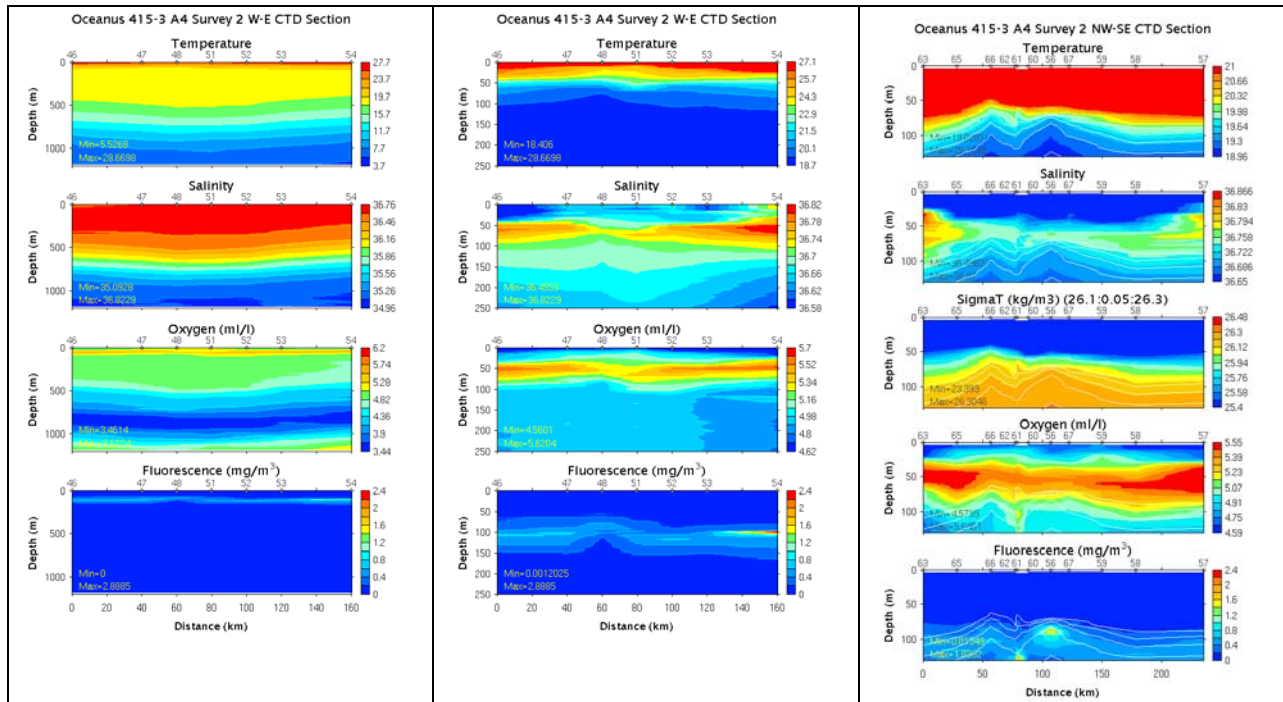


Figure 5: W-E Section across A4. Left: 0-1200m; middle: 0-250m; right: 0-125m. Density contours $\sigma_T = 26.1, 26.15, 26.2, 26.25, 26.3$ are shown in white on the right panel.

9. Water properties on isopycnal surfaces

OC415-1 CTD survey of A4

On all three isopycnal surfaces, waters inside the eddy are generally warmer and saltier than the ambient conditions as defined by a few of the edge stations. On $\sigma_T=26.2$, there is a cold and fresh anomaly located in the inner core of the eddy. Fluorescence peaks in the eddy core where the $\sigma_T=26.25$ isopycnal outcrops into the euphotic zone; this is accompanied by a maximum in oxygen concentration at eddy center which appears to be spreading outward along the isopycnal surface. This oxygen enhancement in the eddy core is also evident on the next lighter isopycnal ($\sigma_T=26.2$), yet fluorescence is enhanced around the periphery of the eddy with a relative minimum located at eddy center. There are at least three possibilities to explain the relative minimum in fluorescence on $\sigma_T=26.2$ at eddy center: (1) nutrients are depleted where the $\sigma_T=26.2$ is shallowest, whereas nutrients are still present where that isopycnal is deeper [testable with nutrient data]; (2) photoadaptation causing less chlorophyll per cell; or (3) fluorescence quenching [only if that station were occupied during the day]. On the next deeper isopycnal ($\sigma_T=26.3$) oxygen is enhanced inside the eddy, perhaps reflecting the higher oxygen content of the mode waters. The nature of the fluorescence enhancement around the periphery of the eddy on $\sigma_T=26.3$ remains enigmatic.

OC415-3 initial core survey and E-W transect of A4

Isopycnal water property distributions share many of the same characteristics observed on OC415-1:

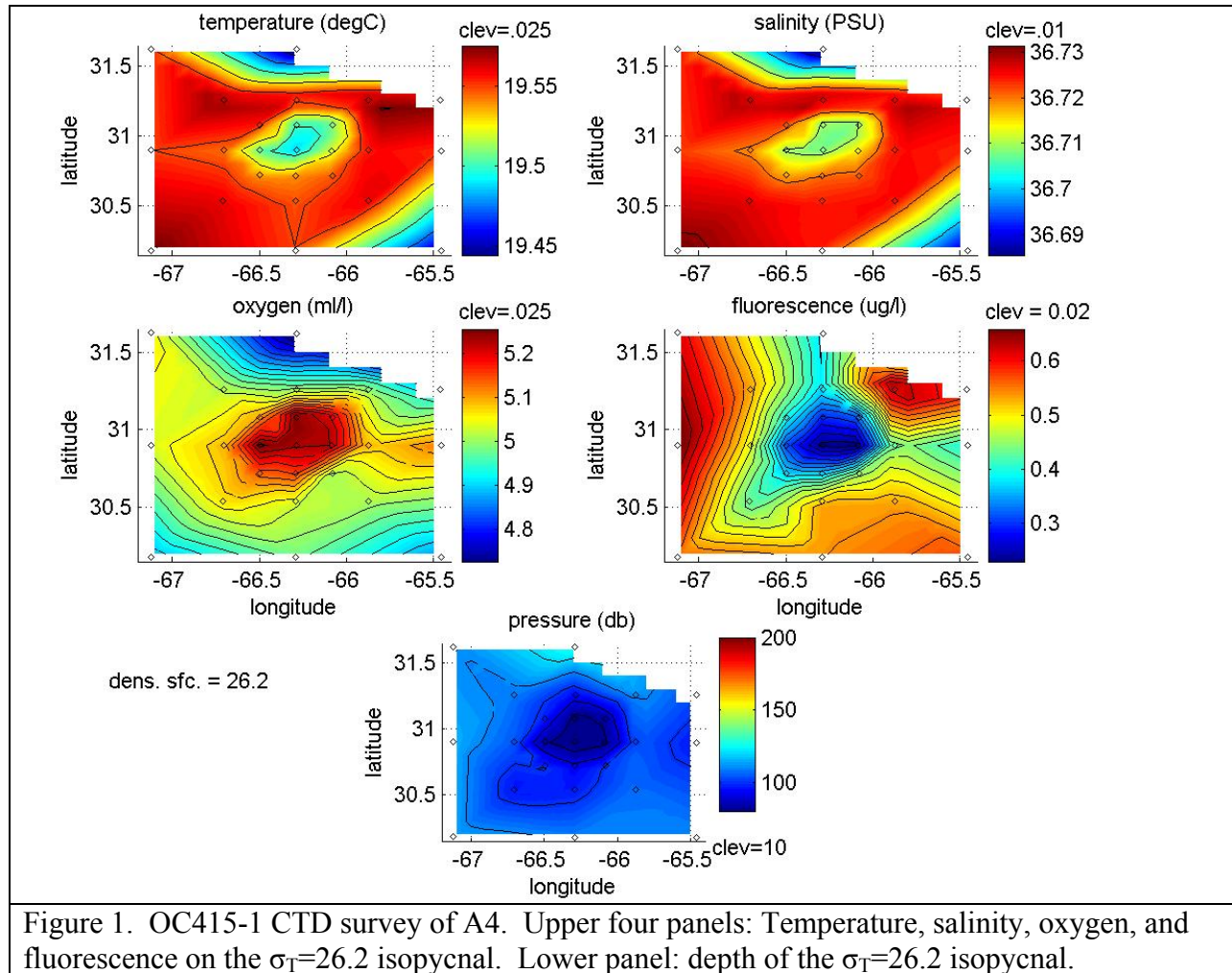
- 1) cold, fresh anomaly at EC on $\sigma_T=26.2$
- 2) warm, salty anomaly in eddy core on $\sigma_T=26.25$, $\sigma_T=26.3$
- 3) oxygen enhancement inside eddy on all three isopycnals
- 4) peak fluorescence at EC on $\sigma_T=26.25$
- 5) local minimum in fluorescence in eddy core on $\sigma_T=26.2$

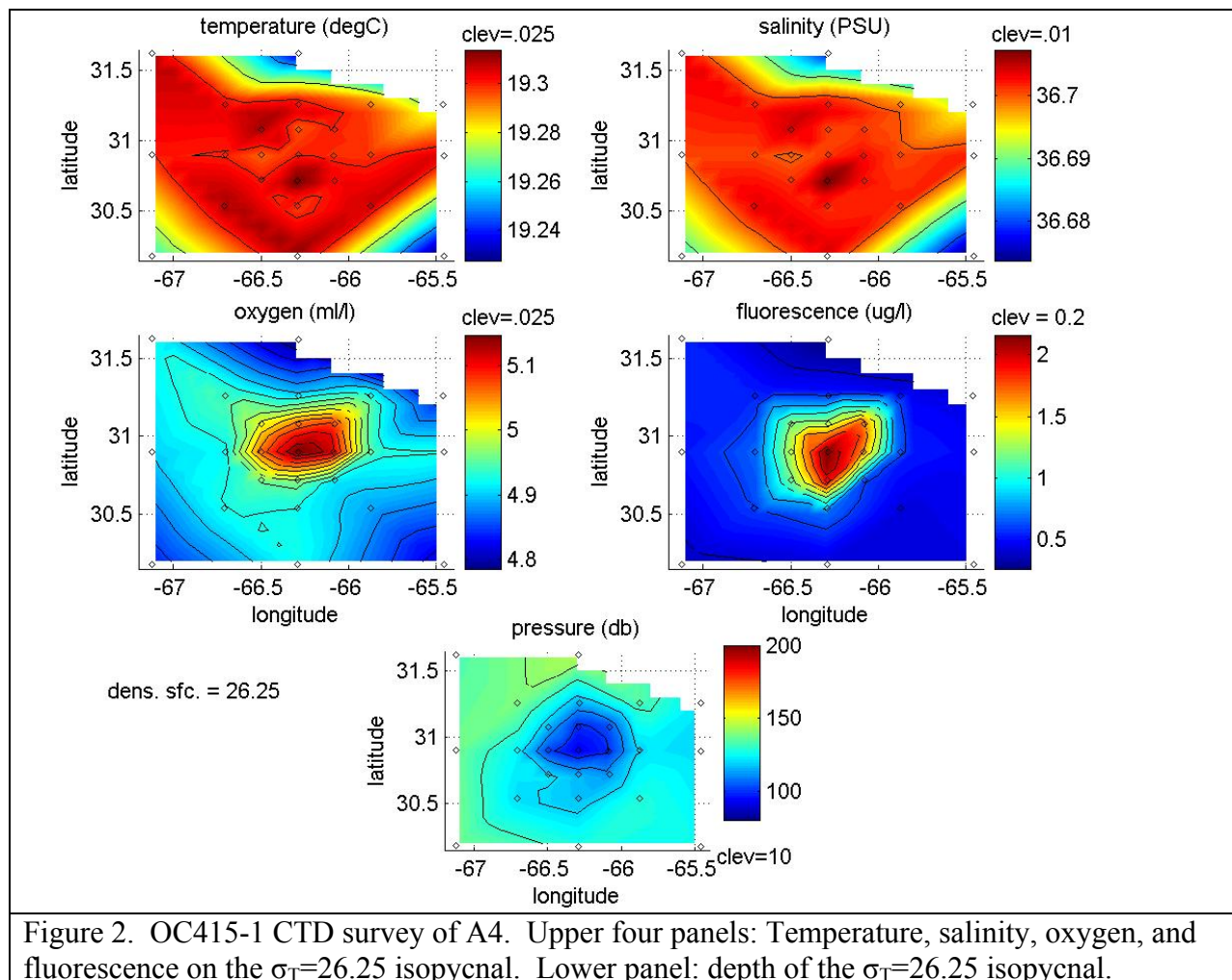
Cruise	Density	Pmin	Pmax	Mean	Std	Median
OC415-1	26.20	71	127	99.4	13.7	101
OC415-1	26.25	92.5	145	120.2	14.0	121
OC415-1	26.30	148	201.5	179.6	12.8	181
OC415-3	26.20	53	125.5	82.6	18.2	81
OC415-3	26.25	65.5	138.5	98.9	19.6	101
OC415-3	26.30	109	179	150.6	18.6	154

Findings:

- 1) bloom occurs where $\sigma_T=26.25$ outcrops into the euphotic zone (EC)
- 2) clear mesoscale signal in oxygen accumulation
 - a. oxygen anomaly at EC associated with bloom on $\sigma_T=26.25$
 - b. oxygen anomaly also present above, on $\sigma_T=26.2$

- 3) distinct water mass characteristics (T,S) in eddy core indicative of propagation as a coherent structure.





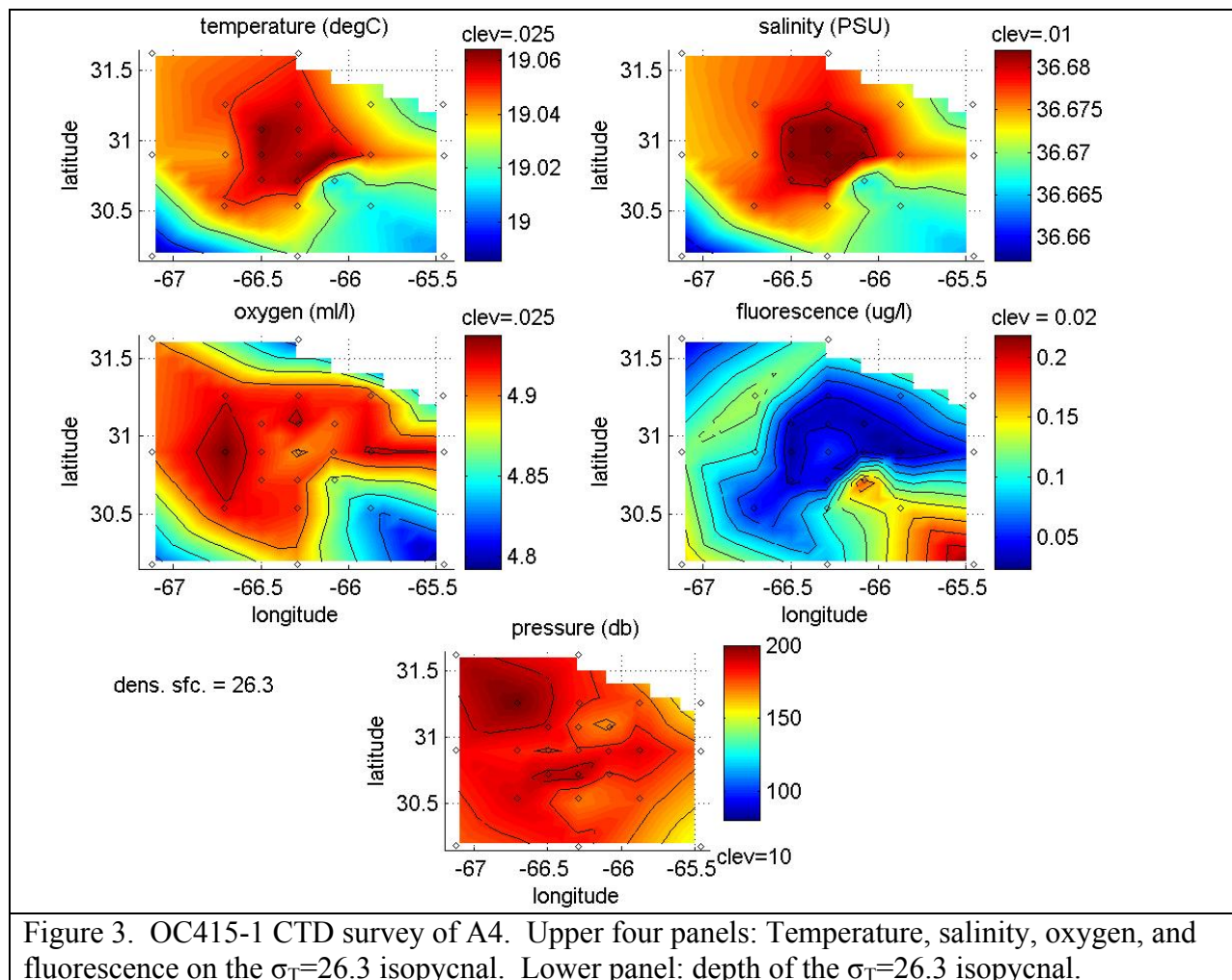
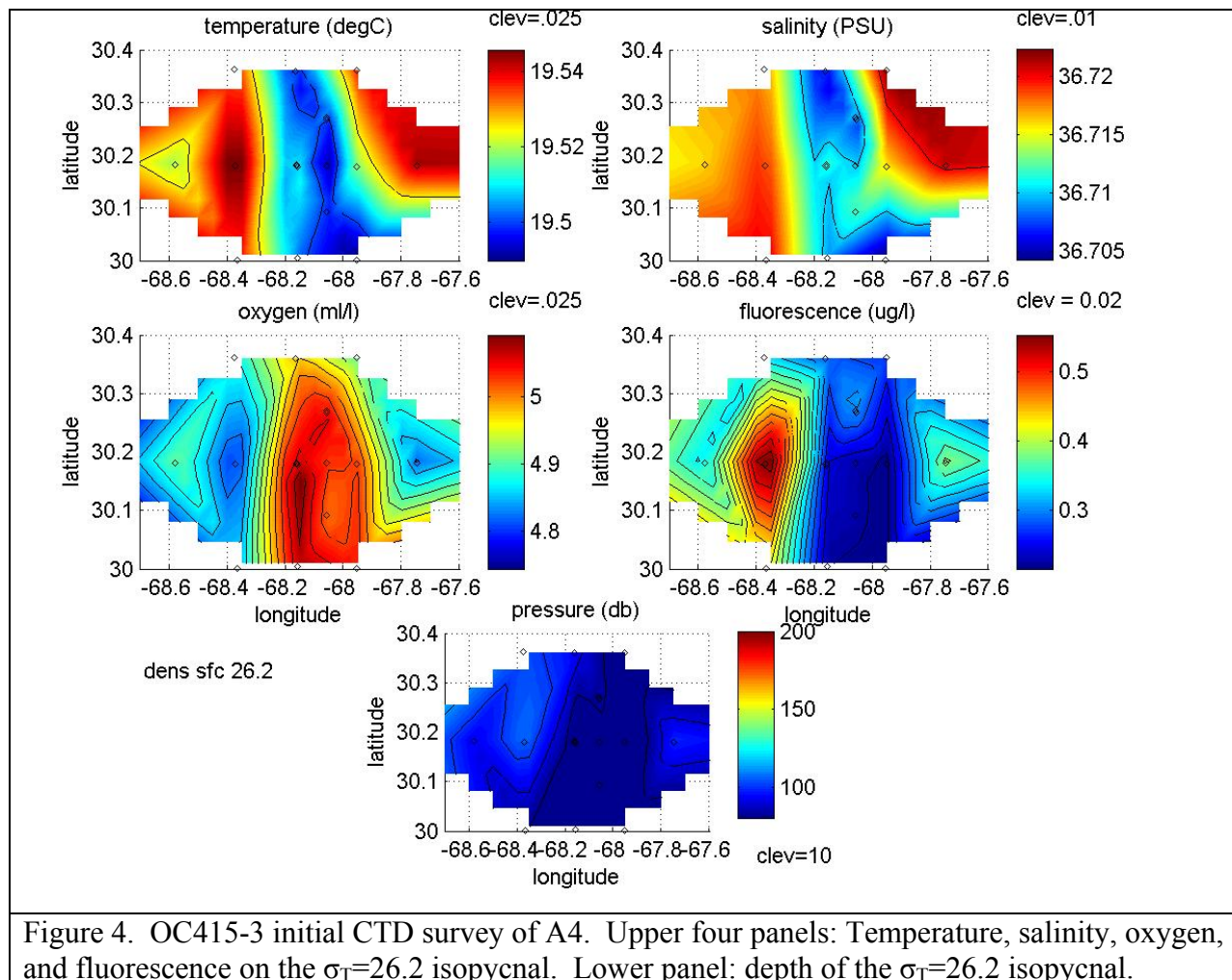


Figure 3. OC415-1 CTD survey of A4. Upper four panels: Temperature, salinity, oxygen, and fluorescence on the $\sigma_T=26.3$ isopycnal. Lower panel: depth of the $\sigma_T=26.3$ isopycnal.



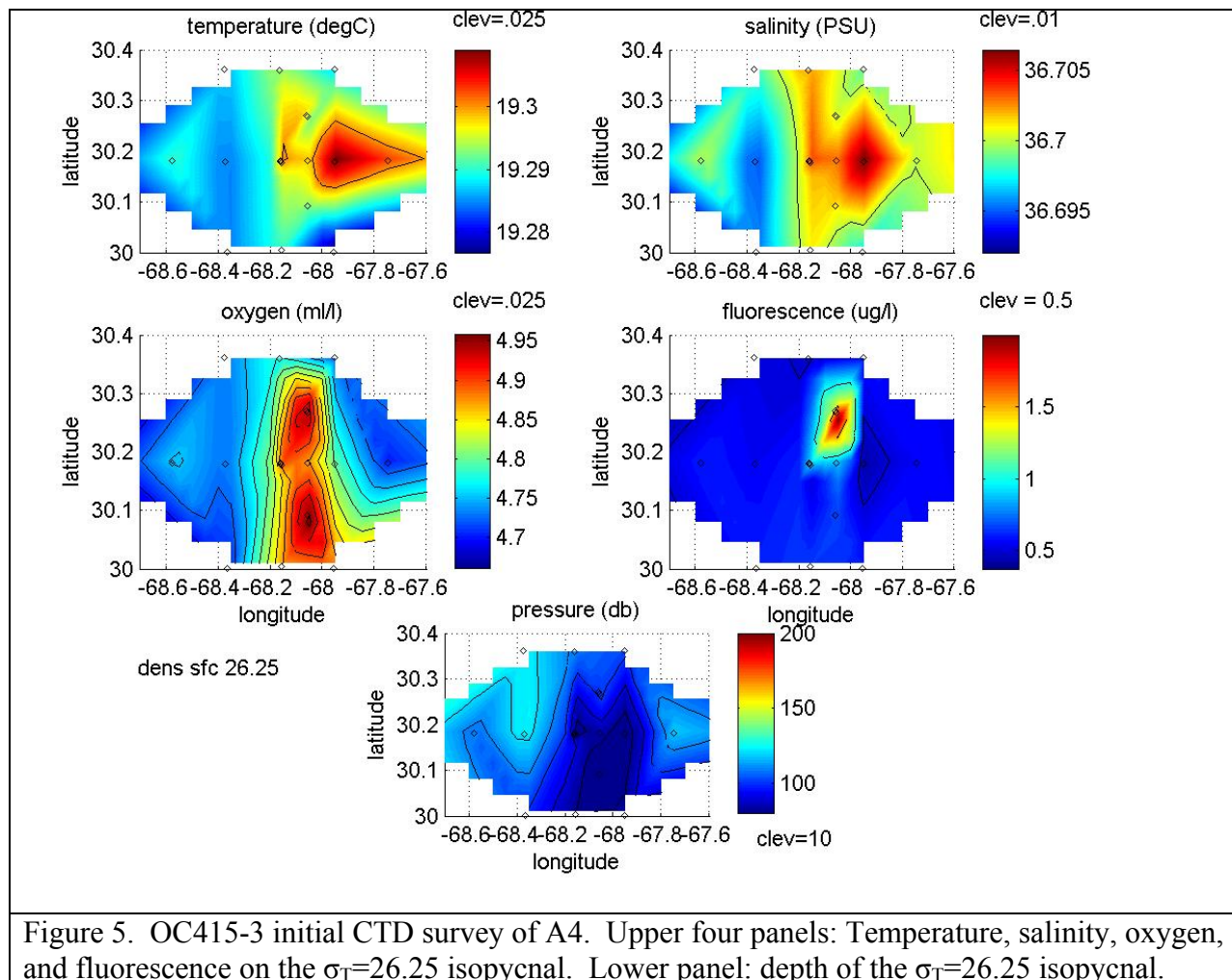


Figure 5. OC415-3 initial CTD survey of A4. Upper four panels: Temperature, salinity, oxygen, and fluorescence on the $\sigma_T=26.25$ isopycnal. Lower panel: depth of the $\sigma_T=26.25$ isopycnal.

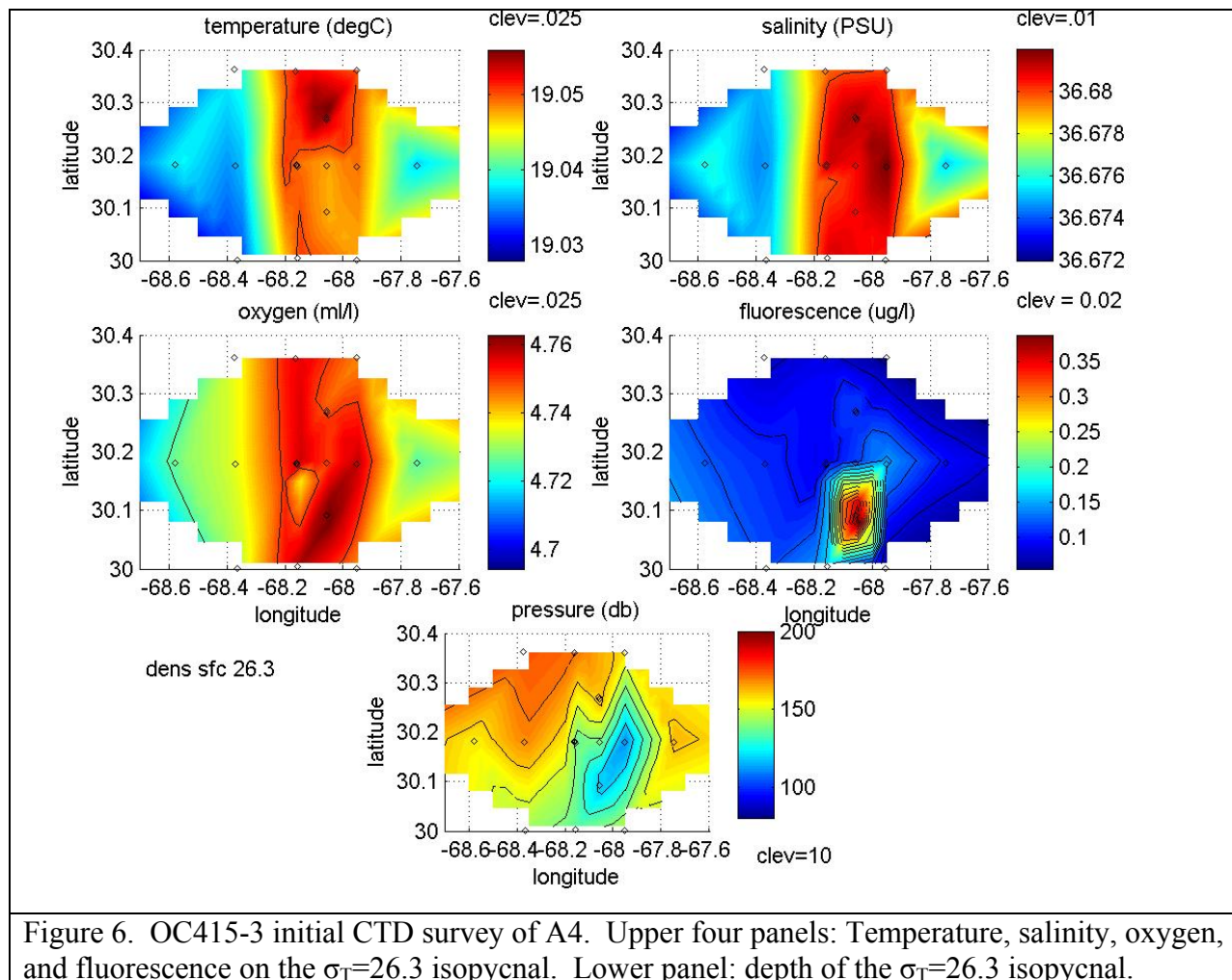
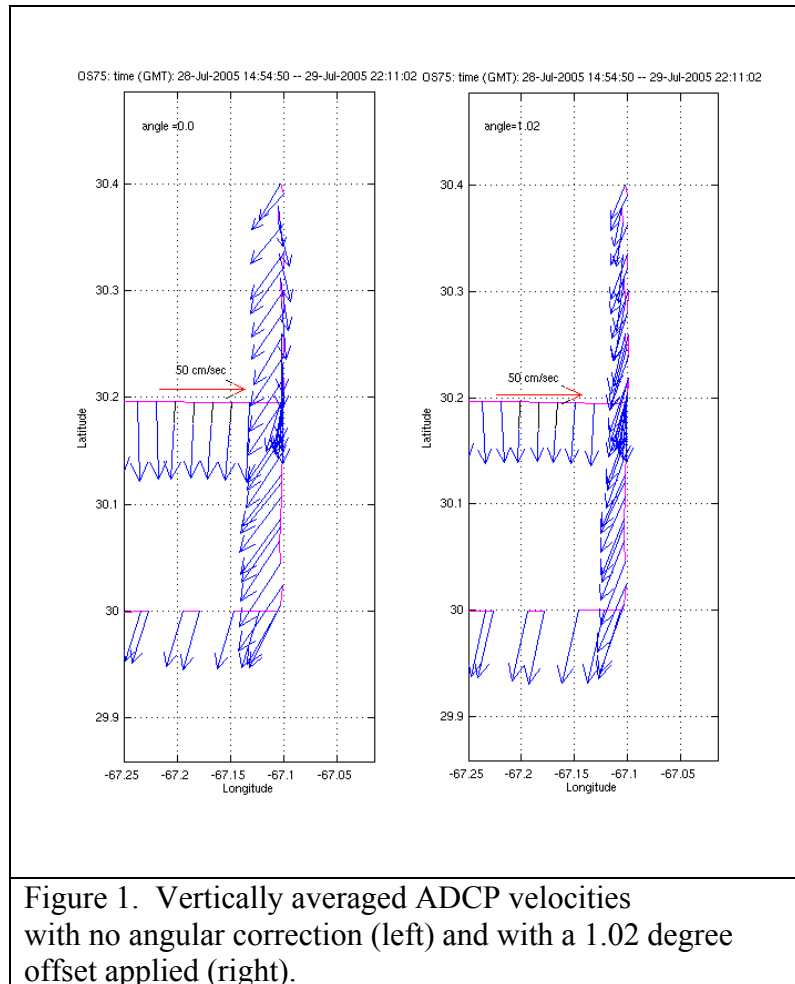


Figure 6. OC415-3 initial CTD survey of A4. Upper four panels: Temperature, salinity, oxygen, and fluorescence on the $\sigma_T=26.3$ isopycnal. Lower panel: depth of the $\sigma_T=26.3$ isopycnal.

10. ADCP data troubleshooting

Jim Ledwell's team noted some suspicious behavior of the OS75 ADCP (Figure 1, left panel). During the south-north-south portion of the trackline, the north-heading track indicates velocities toward the southwest, whereas the south-heading track indicates currents toward the SSE. This behavior is indicative of a transducer alignment error and/or heading error. Examination of the adcpcal.out diagnostic file produced by CODAS suggests a 1.02 degree angular offset. When this offset is applied, it brings the velocities measured during the north-south and south-north tracklines into agreement (Figure 1, right panel).



In order to verify the angular correction, it was applied to two additional segments of data from OC415-2 (Figure 2). In both cases, the velocities appear to be qualitatively improved. In particular, the angular correction lessens sharp gradients in velocity associated with course changes (i.e. the NW corner of the earlier grid [upper panels], and the westernmost point of the later survey [lower panels]). Lastly, the angular correction improves the direct comparison of the OS75 with the NB150 undertaken during OC415-1 (Figure 3). Thus we are satisfied that the 1.02 degree correction is beneficial, and will proceed with that for OC415-3.

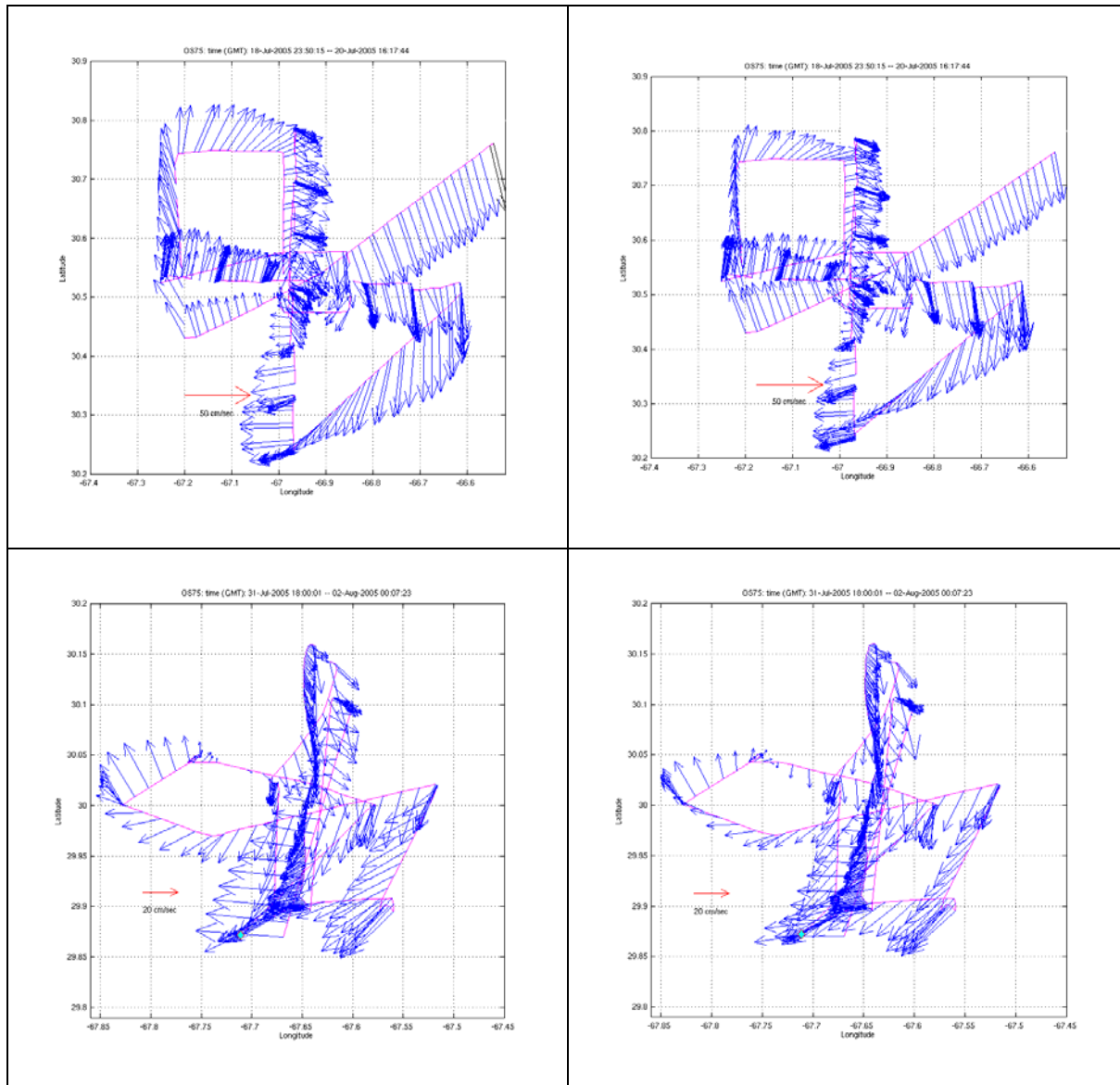


Figure 2. Selected ADCP surveys from OC415-2 without (left panels) and with (right panels) the 1.02 degree angular correction applied.

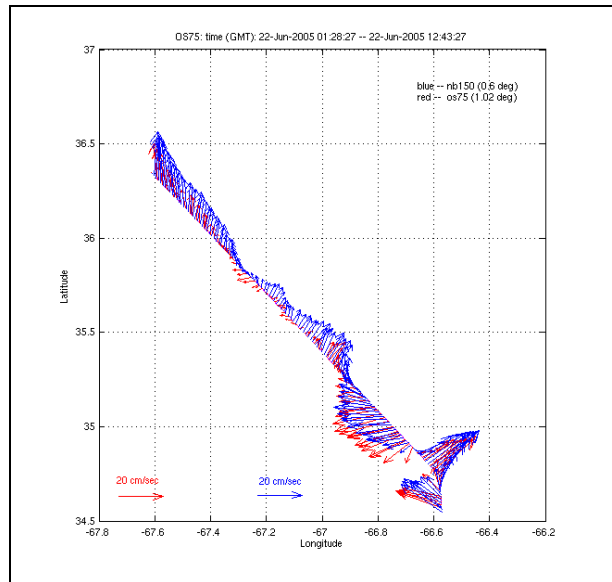


Figure 3. Comparison of vertically averaged velocities (upper 250m) from the OS75 (red) and NB150 (blue) undertaken during OC415-1. The 1.02 degree correction is applied to the OS75 data.

12. Cruise participants

Dr. Dennis McGillicuddy, Chief Scientist, Woods Hole Oceanographic Institution
Mr. Valery Kosnyrev, Woods Hole Oceanographic Institution
Ms. Olga Kosnyreva, Woods Hole Oceanographic Institution
Dr. Laurence Anthony Anderson, Woods Hole Oceanographic Institution
Ms. Ellyn Montgomery, Woods Hole Oceanographic Institution
Ms. Megan Roadman, Bermuda Biological Station for Research
Ms. Sybille Pluinage, Bermuda Biological Station for Research
Mr. Qian Li, RSMAS, University of Miami
Dr. Thomas Spencer Bibby, IMCS, Rutgers University
Ms. Sara Jane Bender, IMCS, Rutgers University
Mr. Donglai Gong, IMCS, Rutgers University
Mr. David William Menzies, University of California Santa Barbara
Dr. William J. Jenkins, Woods Hole Oceanographic Institution
Dr. Sarah Anne Stone, Virginia Institute of Marine Science
Ms. Bethany Rose Eden, Virginia Institute of Marine Science
Mr. Joshua Eaton, Woods Hole Oceanographic Institution
Mr. Patrick Rowe, Woods Hole Oceanographic Institution
Mr. Scott J. McCue, Woods Hole Oceanographic Institution
Mr. Stephan Duller, IMCS, Rutgers University